Transportation Research Part B 56 (2013) 265–293

Contents lists available at ScienceDirect

Transportation Research Part B

journal homepage: www.elsevier.com/locate/trb

The time-dependent pollution-routing problem

Anna Franceschetti [a,*], Dorothée Honhon [a], Tom Van Woensel [a], Tolga Bektaş [b], Gilbert Laporte [c]

[a] School of Industrial Engineering, Eindhoven University of Technology, Eindhoven 5600MB, The Netherlands
[b] Southampton Management School, Centre for Operational Research, Management Science and Information Systems (CORMSIS), University of Southampton, Southampton SO17 1BJ, United Kingdom
[c] Canada Research Chair in Distribution Management, HEC Montréal, Montréal H3T 2A7, Canada

ARTICLE INFO

Article history:
Received 21 March 2013
Received in revised form 12 August 2013
Accepted 13 August 2013

Keywords:
Vehicle routing
Fuel consumption
CO_{2e} emissions
Congestion
Integer programming

ABSTRACT

The Time-Dependent Pollution-Routing Problem (TDPRP) consists of routing a fleet of vehicles in order to serve a set of customers and determining the speeds on each leg of the routes. The cost function includes emissions and driver costs, taking into account traffic congestion which, at peak periods, significantly restricts vehicle speeds and increases emissions. We describe an integer linear programming formulation of the TDPRP and provide illustrative examples to motivate the problem and give insights about the tradeoffs it involves. We also provide an analytical characterization of the optimal solutions for a single-arc version of the problem, identifying conditions under which it is optimal to wait idly at certain locations in order to avoid congestion and to reduce the cost of emissions. Building on these analytical results we describe a novel departure time and speed optimization algorithm for the cases when the route is fixed. Finally, using benchmark instances, we present results on the computational performance of the proposed formulation and on the speed optimization procedure.

1. Introduction

Traffic congestion occurs when the capacity of a particular transportation link is insufficient to accommodate an incoming flow at a particular point in time. Congestion has a number of adverse consequences, including longer travel times and variations in trip duration which result in decreased transport reliability, increased fuel consumption and more carbon dioxide equivalent (CO_{2e}) emissions. The latter measures, for a given mixture and amount of greenhouse gas, the amount of CO_2 that would have the same global warming potential (GWP) (Wikipedia, 2013). It is known that CO_{2e} emissions are proportional to fuel consumption and depend on vehicle speed. Heavy congestion results in low speeds with fluctuations, often accompanied by frequent acceleration and deceleration, and greatly contributes to CO_{2e} emissions (Barth and Boriboonsomsin, 2008). According to the International Road Transport Union (IRU), around 100 billion liters of wasted fuel, or 250 billion tonnes of CO_{2e}, were attributed to traffic congestion in the United States in 2004 (IRU, 2012). Noise is another externality resulting from congestion. In particular, noise from a vehicle's power unit comprising the engine, air intake and exhaust becomes dominant at low speeds of 15–20 mph and at high acceleration rates of 2 m/s^2, as reported by the World Business Council for Sustainable Development (2004) (Knight, 2004). Congestion is at its highest during rush hour, which typically lasts from 6am or 7am to 9am or 10am in the morning, although this varies from one city to another, e.g., 6am–9am in Sydney, Brisbane and Melbourne, and 4am–9am in New York City (Wikipedia, 2012).

* Corresponding author. Tel.: +31 40 2472601.
E-mail address: A.Franceschetti@tue.nl (A. Franceschetti).

0191-2615/$ - see front matter © 2013 Elsevier Ltd. All rights reserved.
http://dx.doi.org/10.1016/j.trb.2013.08.008

Our aim is to study the effect of congestion and CO_{2e} emissions within the context of the Vehicle Routing Problem (VRP), defined as the problem of routing a fleet of vehicles to serve a set of customers subject to various constraints, such as vehicle capacities (see e.g., Cordeau et al., 2007). Previous VRP research assumes constant vehicle speed, which is not realistic for most practical applications. Van Woensel et al. (2001) show that solving the VRP under this assumption can lead to deviations of up to 20% in CO_{2e} emissions for gasoline vehicles on an average day and up to 40% in congested traffic. Indeed, vehicle speed varies throughout the day (Van Woensel et al., 2008), which affects CO_{2e} emissions. Maden et al. (2010) present an approach for the time-dependent vehicle routing problem which allows for the planning of more reliable routes and schedules. It is based on a tabu search algorithm, which minimizes the total travel time and reduces emissions by avoiding congestion. The authors have applied this algorithm to a real-life case study and have obtained reductions of about 7% in CO_{2e} emissions.

Accounting for emissions in the context of the VRP is relatively new. For a general introduction to the topic we refer the reader to Sbihi and Eglese (2007). Figliozzi (2010) presents the emissions minimizing VRP (EVRP), a variant of the time-dependent VRP (TDVRP) with time windows, which takes into account congestion so as to minimize speed-dependent CO_{2e} emissions, using a function described by Hickman et al. (1999). The EVRP is modeled on a partition of the working time, and a set of speeds on each arc (i,j) of the network is defined as a function of the departure time from node i. A model for the EVRP described by Figliozzi (2010) uses route and departure times as decision variables, but the model also optimizes speeds as a consequence of the objective function. Conrad and Figliozzi (2010) and Figliozzi (2011) present results related to a variant of the EVRP on a case study in Portland, Oregon, where scenarios with and without congestion are considered. These papers focus on finding approximate, rather than optimal, solutions to the problems, and hence heuristic algorithms are used to generate solutions. Jabali et al. (2012) take a similar approach by using the same emissions function in a formulation of the time-dependent VRP (without time windows), with speed as an additional decision variable. Travel times are modeled by partitioning the planning horizon into two parts, where one part corresponds to a peak period in which there is congestion and the vehicle speed is fixed, whereas the other part assumes free-flow speeds which can be optimized. Jabali et al. (2012) describe a tabu search heuristic for this problem.

Another contribution along these lines is due to Bektaş and Laporte (2011) who present the Pollution-Routing Problem (PRP) as an extension of the classical Vehicle Routing Problem with Time Windows (VRPTWs). The PRP consists of routing a number of vehicles to serve a set of customers within preset time windows, and determining their speed on each route segment, so as to minimize a function comprising emissions and driver costs. The emissions function used within the PRP is based on a comprehensive emissions model for heavy-duty vehicles described by Barth et al. (2005), and differs from previous work in that it allows to optimize *both* load and speed. The PRP formulation described by Bektaş and Laporte (2011) considers only free-flow speeds of 40 km/h or higher. Demir et al. (2012) extend the PRP formulation to take into account lower speeds, but without looking at congestion *per se*, and describe a heuristic that can solve large-size instances.

A common assumption in the VRPTW is to allow arrival at a customer location before the opening of the time window, but service can only start within the time window. None of the work mentioned above has allowed for idle waiting after service completion as a strategy to avoid congestion. We incorporate, for the first time, congestion into the PRP framework so as to adequately account for the adverse effects of low speeds caused by congestion, and we make use of the "idle waiting" strategy.

We introduce the Time-Dependent Pollution-Routing Problem (TDPRP), which extends the PRP by explicitly taking into account traffic congestion, and we describe an integer linear programming formulation of the TDPRP where the vehicles speeds are optimized among a set of discrete values. We also provide an analytical characterization of the optimal solutions for a single-arc version of the problem and describe a procedure for optimizing the departure times and speeds when the route is fixed and speed is a continuous variable. Finally we report computational experiments with the integer programming formulation and the speed optimization procedure on benchmark instances.

The contribution of this paper is multi-fold and can be stated as follows: (i) we break away from the literature on congestion-aware VRP by using a comprehensive emissions function which includes factors such as load and speed, (ii) we demonstrate how the total travel cost can be significantly reduced by allowing the vehicle to wait at the depot or at a customer node, after the service has been completed, (iii) we propose an integer linear programming formulation of the TDPRP which computationally improves upon the PRP formulation, (iv) we generate new insights on the trade-off between emissions cost and driver wage, and (v) we develop a novel algorithm to optimize departure times and travel speeds on a fixed vehicle route.

It should be noted at this point that all results derived here also hold for the special case of zero pollution costs. In other words, our results apply to the problem of optimizing vehicle speeds and departure times in contexts characterized by driver costs, time windows and traffic congestion only.

The remainder of the paper is structured as follows. The next section presents a formal description of the TDPRP and our general modeling framework. Section 3 provides illustrative examples to motivate the problem. Section 4 describes an integer linear programming formulation of the TDPRP. A complete analytical characterization of the optimal solutions for a single-arc version of the problem is provided in Section 5. In Section 6, we describe a procedure to optimize departure times and speeds on a fixed route. Computational results obtained on benchmark instances with the proposed TDPRP formulation and the speed optimization procedure are presented in Section 7. Conclusions follow in Section 8.

For the sake of conciseness, all proofs are provided in Appendix C.

2. Problem description

The TDPRP is defined on a complete graph $G = \{N, A\}$ where N is the set of nodes, 0 is the depot, $N_0 = N \setminus \{0\}$ is the set of customers, and A is the set of arcs between every pair of nodes. The distance between two nodes $i \neq j \in N$ is denoted by d_{ij}. A homogeneous fleet of K vehicles, each with a capacity limit of Q units, is available to serve all customers, where each customer $i \in N_0$ has a non-negative demand q_i. To each customer $i \in N_0$, corresponds a service time h_i and a hard time window $[l_i, u_i]$ in which service must start. In particular, if a vehicle arrives at node i before l_i, it waits until time l_i to start service. Without loss of generality we assume that the vehicle can depart from the depot at time zero (we relax this assumption in Sections 5 and 6).

The following sections present the way in which time-dependency and congestion are modeled in the TDPRP, and how CO_{2e} emissions are calculated.

2.1. Time-dependency

In the PRP (Bektaş and Laporte, 2011), the travel time of a vehicle depends only on distance and speed, and the latter can be chosen freely. In the TDPRP, the speed also depends on the departure time of the vehicle because it is constrained during periods of traffic congestion. Here, we make use of time-dependent travel times and model traffic congestion using a two-level speed function as in Jabali et al. (2012). We assume there is an initial period of congestion, lasting a units of time, followed by a period of free-flow. This modeling framework is suitable for routing problems which must be executed in the first half of a given day, e.g., starting from a peak-morning period where traffic congestion is expected, and following which it will dissipate. In the peak-period, the vehicle travels at a *congestion speed* v_c whereas in the period that follows, it is only limited by the speed limits v_{min} and v_{max}, meaning that the vehicle drives at *free-flow speed* $v_f \in [v_{min}, v_{max}]$. These bounds may be explicitly imposed by the driving code or may implicitly result from traffic regulations such as a ban on overtaking for heavy vehicles.

For practical reasons we assume that the speed v_c and the time a are constants which can be extracted from archived travel data (e.g., Hansen et al., 2005) and that the same values hold between every pair of locations.

To model time-dependency, consider two locations spaced out by a distance of d. Let $T(w, v_f)$ denote the travel time of a vehicle between the two locations, that is the time spent by the vehicle on the road depending on its departure time w from the first location, and the chosen free-flow speed v_f. It can be calculated using the following formulation proposed by Jabali et al. (2012):

$$T(w, v_f) = \begin{cases} \frac{d}{v_c} & \text{if } w \leqslant \left(a - \frac{d}{v_c}\right)^+ \\ \frac{v_f - v_c}{v_f}(a - w) + \frac{d}{v_f} & \text{if } \left(a - \frac{d}{v_c}\right)^+ < w < a \\ \frac{d}{v_f} & \text{if } w \geqslant a. \end{cases} \tag{1}$$

The calculation of $T(w, v_f)$ suggests that the planing horizon can be divided into three consecutive time regions in terms of the departure time w, as follows:

- The first one $w \in \left[0, \left(a - \frac{d}{v_c}\right)^+\right]$ is called the *all congestion* region: the vehicle leaving the first location within this region makes the entire trip during the congestion period and arrives at the second location after d/v_c units of time.
- The second one $w \in \left[\left(a - \frac{d}{v_c}\right)^+, a\right]$, is called the *transient* region: the vehicle leaving within this region traverses a distance of length $(a - w)v_c$ at speed v_c and the remaining distance of length $d - (a - w)v_c$ at the chosen free-flow speed v_f.
- The last one $w \in [a, \infty)$, is called the *all free-flow* region, in which the vehicle makes the entire trip at the free-flow speed v_f and completes the journey in d/v_f units of time.

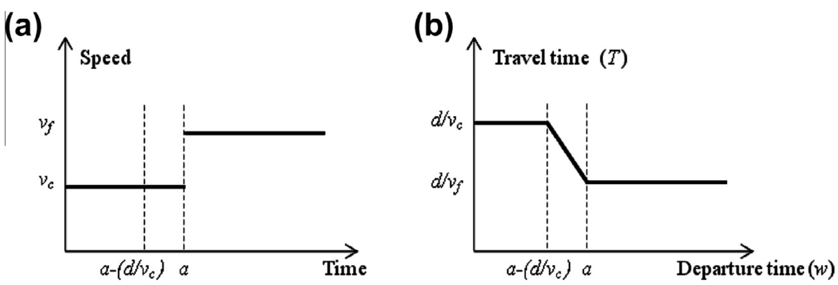

Fig. 1. Time-dependent (a) speed and (b) travel time profiles.

Fig. 1(a) shows the speed of a vehicle as a function of time for $v_f > v_c$. Fig. 1(b) shows how T varies with the departure time w given free-flow speed v_f.

2.2. Modeling emissions

Our modeling of emissions follows the same approach as in Bektaş and Laporte (2011). Here we provide a brief exposition for the sake of completeness. Since CO_{2e} emissions are directly proportional to the amount of fuel consumed, we use the fuel use rate as a proxy to estimate the total amount of CO_{2e} emissions. To calculate fuel consumption, we use the *comprehensive emissions model* of Barth et al. (2005) and Barth and Boriboonsomsin (2008), according to which the instantaneous fuel use rate, denoted FR (l/s), when traveling at a constant speed v (m/s) with load f (kg) is estimated as

$$FR = \frac{\xi}{\kappa\psi}\left(kN_eV + \frac{0.5C_d\rho Av^3 + (\mu + f)v(g\sin\phi + gC_r\cos\phi)}{1000\varepsilon\varpi}\right), \tag{2}$$

where ξ is fuel-to-air mass ratio, κ is the heating value of a typical diesel fuel (kJ/g), ψ is a conversion factor from grams to liters from (g/s) to (l/s), k is the engine friction factor (kJ/rev/l), N_e is the engine speed (rev/s), V is the engine displacement (l), ρ is the air density (kg/m^3), A is the frontal surface area (m^2), μ is the vehicle curb weight (kg), g is the gravitational constant (equal to 9.81 m/s^2), ϕ is the road angle, C_d and C_r are the coefficient of aerodynamic drag and rolling resistance, ε is vehicle drive train efficiency and ϖ is an efficiency parameter for diesel engines. Using $\alpha = g\sin\phi + gC_r\cos\phi$, $\beta = 0.5C_dA\rho$, $\gamma = 1/(1000\varepsilon\varpi)$ and $\lambda = \xi/\kappa\psi$, (2) can be simplified as

$$FR = \lambda(kN_eV + \gamma(\beta v^3 + \alpha(\mu + f)v)). \tag{3}$$

The total amount of fuel used, denoted F (l), for traversing a distance d (m) at *constant* speed v (m/s) with load f (kg) is equal to the fuel rate multiplied by the travel time d/v:

$$F = \lambda\left(kN_eV\frac{d}{v} + \gamma\beta dv^2 + \gamma\alpha(\mu + f)d\right). \tag{4}$$

Expression (4) contains three terms in the parentheses. We refer to the first term, namely kN_eVd/v, as the *engine module* which is linear in the travel time. The second term, $\gamma\beta dv^2$, is called the *speed module*, which is quadratic in the speed. The last term, $\gamma\alpha(\mu + f)d$, is the *weight module*, which is independent of travel time and speed. Fig. 2 shows the relationship between F and v for a vehicle traveling a distance of 100 km. Other parameters used in generating the figure are given in Table 1.

Fig. 2 shows a U-shape curve between fuel consumption and speed, which is consistent with the behavior of functions suggested by other authors (e.g., Demir et al., 2011), confirming that low speeds (as in the case of traffic congestion) lead to very high fuel use rate. The figure also shows the engine module as the main driver of this trend, which contributes considerably to the increase in the amount of emissions at low speeds.

To model the emissions in a time-dependent setting, we rewrite the fuel consumption function F as a function of the departure time w and the free-flow speed v_f on a given arc of length d. If a vehicle traverses the arc in the *all congestion* region, then

$$F(w, v_f) = \lambda\left[kN_eVT(w, v_f) + \gamma\beta T(w, v_f)v_c^3 + \gamma\alpha(\mu + f)d\right].$$

Similarly, in the *all free-flow* region,

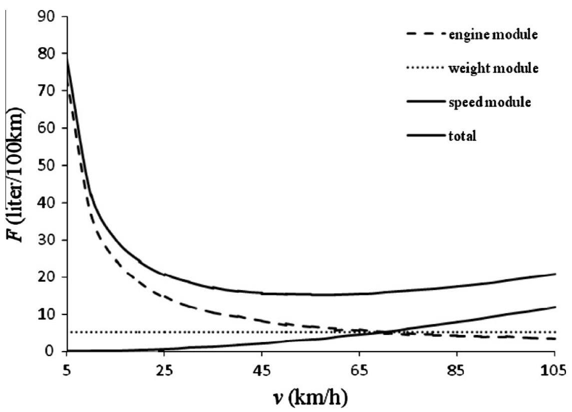

Fig. 2. Fuel use rate F as a function of speed v.

Table 1
Setting of vehicle and emissions parameters.

Notation	Description	Value
ξ	Fuel-to-air mass ratio	1
κ	Heating value of a typical diesel fuel (kJ/g)	44
ψ	Conversion factor (g/l)	737
k	Engine friction factor (kJ/rev/l)	0.2
N_e	Engine speed (rev/s)	33
V	Engine displacement (l)	5
ρ	Air density (kg/m^3)	1.2041
A	Frontal surface area (m^2)	3.912
μ	Curb-weight (kg)	6350
g	Gravitational constant (m/s^2)	9.81
ϕ	Road angle	0
C_d	Coefficient of aerodynamic drag	0.7
C_r	Coefficient of rolling resistance	0.01
ε	Vehicle drive train efficiency	0.4
ϖ	Efficiency parameter for diesel engines	0.9
f_c	Fuel price per liter (£)	1.4
d_c	Driver wage (£/s)	0.0022

$$F(w, v_f) = \lambda\Big[kN_eVT(w, v_f) + \gamma\beta T(w, v_f)v_f^3 + \gamma\alpha(\mu + f)d\Big].$$

When a vehicle traverses the arc in the *transient* region, the speed module needs to be split into two terms since the speed changes before and after the end of the congestion period. In this case

$$F(w, v_f) = \lambda\Big[kN_eVT(w, v_f) + \gamma\beta\Big[(a - w)v_c^3 + (w + T(w, v_f) - a)v_f^3\Big] + \gamma\alpha(\mu + f)d\Big],$$

where $a - w$ is the time spent in congestion and $w + T(w, v_f) - a$ is the time spent driving at free-flow speed.

In general, let $T^c(w) = \min\{(a - w)^+, d/v_c\}$ be the time spent by the vehicle in congestion and $T^f(w, v_f) = [d - (a - w)^+ v_c]^+/v_f$ be the time spent driving at the free-flow speed. We have $T(w, v_f) = T^c(w) + T^f(w, v_f)$ and we can write

$$F(w, v_f) = \lambda kN_eVT(w, v_f) + \lambda\gamma\beta\Big[T^c(w)v_c^3 + T^f(w, v_f)v_f^3\Big] + \lambda\gamma\alpha(\mu + f)d.$$

2.3. Aim of the TDPRP

In the TDPRP, the total travel cost function is composed of the cost of the vehicle emissions and the driver cost for each arc in the network. Let f_c denote the fuel price per liter and let d_c denote the wage rate for the drivers of the vehicles. In this paper we assume that the CO_{2e} emissions cost is equal to the fuel cost. In practice, we could modify f_c to include the cost of emissions. However, there is considerable debate on the price of CO_{2e} and the method used to estimate it is rather subjective (see the survey paper by Tol (2005) gathering 103 estimates of the marginal damage costs of CO_{2e} emissions), so we have decided not to include it in our numerical calculations.

We consider two ways of calculating the total time for which the driver is paid, which we call *driver wage policies*: (i) the driver of each vehicle is paid from the beginning of the time horizon until returning back to the depot, or (ii) the driver is paid only for the time spent away from the depot, i.e., either en-route or at a customer. The difference between policies (i) and (ii) is that the driver is not paid for time spent waiting at the depot under policy (ii); in practice, the driver is asked to report to work later than at the start of the time horizon.

The aim of the TDPRP is to determine a set of routes, starting and ending at the depot, the speeds on each leg of the routes and departure times from each node so as to minimize the total travel cost. We provide an expression for the cost function in Section 4 and one for the special case of a network with only one arc in Section 5.

In the next section we present a number of numerical examples which illustrate the trade-offs involved in this model. In particular, we outline an important feature of the TDPRP, i.e., that it may be optimal to wait at a node, even after the service is completed, in order to reduce the time spent driving in congestion. Similarly, it may also be optimal for the vehicles not to leave the depot at the start of the time horizon. Hence, the driver's time at a customer can be spent (i) waiting for the start of service in the case of an early arrival—we call this the *pre-service* wait, (ii) serving the customer, or (iii) waiting after service is completed and before departing to the next customer or back to the depot—we call this the *post-service* wait.

3. Examples

The purpose of this section is twofold. We first investigate the impact of considering traffic congestion on the routing and scheduling planning activities. We then compare the two driver wage policies, namely paying the drivers from the beginning

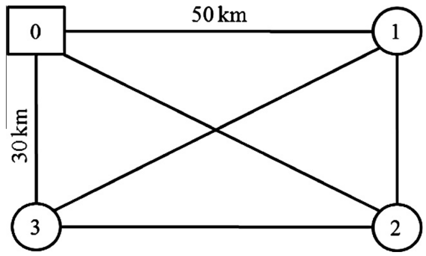

Fig. 3. Sample four-node instance.

of the time horizon or from their departure time from the depot. In both cases, we analyze a four-node network where node 0 is the depot at which a single vehicle is based, and {1,2,3} is the set of customers. The network is depicted in Fig. 3. Every arc has the same two-level speed profile consisting of an initial congestion period which lasts a seconds, followed by a free-flow period. In the examples below, the congestion speed v_c is set to 10 km/h, the minimum speed limit v_{min} to 50 km/h and the maximum speed limit v_{max} to 110 km/h. The examples differ with respect to the driver wage policy and the time windows at the customer nodes, which are given above each table. We assume that demand and service time at each customer node are zero. The assumption on the demand values entails no loss of generality given that the weight module does not depend on the vehicle speed, as shown in Section 2.2. The parameters used to calculate the total cost function, which are reported in Table 1, are taken from Demir et al. (2012).

3.1. Impact of traffic congestion

We consider four examples. In each one, we minimize the total travel cost using two different approaches. In the *time-independent* approach, we ignore traffic congestion when planning the vehicle route and schedule, that is, we assume that the vehicle can always drive at the chosen free-flow speed on each arc of the network. Let S_N denote the solution of the time-independent approach. In the *time-dependent* approach, we account for traffic congestion by solving the TDPRP, the solution of which we denote by S_D. However, the costs for both solutions (denoted by $TC(S_N)$ and $TC(S_D)$) are evaluated under traffic congestion. Since S_D is optimal under traffic congestion, it follows that $TC(S_D) \leqslant TC(S_N)$, and the difference in cost between the two solutions represents the value of incorporating traffic congestion information in the decision making process. In the example below, the length of the congestion period is equal to 14,400 s.

Example 1: Post-service wait at depot

This example shows that ignoring traffic congestion when planning the route and schedule of the vehicle can lead to a substantial increase in costs. It also shows that adding waiting time at the depot can be used as an effective strategy to mitigate the effect of congestion and reduce the total travel cost. We assume no service time windows at customer nodes: $l_1 = l_2 = l_3 = 0$, and $u_1 = u_2 = u_3 = \infty$. The driver is paid from the beginning of the time horizon.

The solutions to the time-independent and time-dependent approaches are displayed in Table 2. For each solution, the table reports (i) the set of traversed arcs in chronological order from top to bottom under column Arc, (ii) the speeds(s) at which each arc is traversed (for an arc traversed during the *transient* region, both the congestion speed and free-flow speed are reported), (iii) the departure time from the origin node, (iv) the post-service waiting time at the origin node, i.e. the additional time that the driver intentionally waits once the service is completed before leaving a node (at the depot the waiting time is equal to the departure time), (v) the emissions cost F, (vi) the driver cost W and (vii) the total cost TC.

From Table 2, we see that the two solutions yield the same optimal tour (0,1,2,3,0) and the same set of optimal free-flow speed levels (75.34 km/h on each arc). The difference between the two solutions lies in the fact that the vehicle leaves the depot at time zero in S_N but waits until the end of the congestion period in S_D. Thus, S_D yields a higher driver cost but this

Table 2
Comparison of S_N and S_D in Example 1.

Arc	S_N						Arc	S_D					
	Speed (km/h)	Departure time (s)	Waiting time (s)	F (£)	W (£)	TC (£)		Speed (km/h)	Departure time (s)	Waiting time (s)	F (£)	W (£)	TC (£)
(0,1)	10, 75.34[a]	0	0	25.86	32.73	58.59	(0,1)	75.34	14,400	14,400	11.47	36.94	48.40
(1,2)	75.34	14877.8	0	6.88	3.15	10.03	(1,2)	75.34	16789.2	0	6.88	3.15	10.03
(2,3)	75.34	16311.3	0	11.47	5.26	16.72	(2,3)	75.34	18222.7	0	11.47	5.26	16.72
(3,0)	75.34	18700.5	0	6.88	3.15	10.03	(3,0)	75.34	20611.8	0	6.88	3.15	10.03
Total				51.09	44.29	95.38					36.70	48.50	85.20

[a] *Transient* region.

increase is more than compensated by an emissions cost saving, yielding a 10.67% total cost saving over S_N (85.20 instead of 95.38).

Example 2: Post-service wait at a customer node

This example shows that ignoring traffic congestion can lead to a significant cost increase when the schedule fails to include post-service wait times which help to mitigate the negative impacts of traffic congestion on emissions costs. It also highlights the difference between pre-service and post-service waits. We assume the following service time windows (in s) at customer nodes: $l_1 = 15{,}000$, $l_2 = 0$, $l_3 = 11{,}000$, $u_1 = u_2 = \infty$, $u_3 = 12{,}000$. The driver is paid from the beginning of the time horizon. The solutions to the time-independent and time-dependent approaches are displayed in Table 3.

In this example, S_N and S_D yield the same optimal route but different schedules. In both solutions, the time at which the driver arrives at node 3 is 3200 s before the lower limit of the time window, hence there is a positive pre-service wait time at that node. In the S_N solution, the vehicle leaves immediately after serving customer 3, while in the S_D solution it waits until the end of the traffic congestion. Hence, the pre-service and post-service waiting times at node 3 are both positive in S_D. This change in the schedule leads to cost savings of 2.56% over the time-independent solution. From this example, it can be seen that, while pre-service wait times can occur in S_N and S_D, post-service wait times are strategic decisions motivated by the impact of congestion and in this example only occur in S_D, when the driver is paid from the beginning of the time horizon.

Example 3: Late deliveries due to congestion

This example shows that ignoring traffic congestion can prevent the driver from delivering within the set time windows because he chose a suboptimal route and suboptimal free-flow speeds. This can have significant negative consequences in terms of future business profitability. We assume the following service time windows (in seconds) at customer nodes: $l_1 = l_2 = l_3 = 0$, $u_2 = 15{,}500$ and $u_1 = u_3 = \infty$. The driver is paid from the beginning of the time horizon. The solutions to the time-independent and time-dependent approaches are displayed in Table 4.

We see from Table 4 that the optimal tour for S_N is (0, 1, 2, 3, 0) and the optimal free-flow speed, without congestion, is 75.34 km/h for every arc. Under congestion, however, the vehicle is only able to reach customer 2 after $14877.8 + (30/75.34)3600 = 16311.3$ s, that is, with a 13.5 min delay with respect to the upper time window limit. Because of this delay, S_N is infeasible in the presence of traffic congestion. The optimal route (0, 2, 1, 3, 0) under S_D is different and so are the free-flow speeds (106.02 km/h on the first arc and 75.34 km/h afterwards). By accounting for traffic congestion, the planner realizes that the driver must go to customer 2 first. It does so after an initial waiting time of 5070.96 s at the depot, and then proceeds at a speed of 106 km/h to reach customer 2, exactly at the upper limit of its time window, at 15,500 s.

Example 4: Reduction of driver and emissions costs

This example shows that S_N and S_D solutions can both have strategic wait times but for reasons which are different from those mentioned above. We assume the following service time windows (in seconds) at customer nodes: $l_1 = 19{,}000$, $l_2 = 0$, $l_3 = 11{,}000$, $u_1 = u_2 = u3 = \infty$. Contrary to the previous three examples, the driver is now paid from his departure time. The solutions to the time-independent and time-dependent approaches are displayed in Table 5.

Table 3
Comparison of S_N and S_D in Example 2.

Arc	S_N						Arc	S_D					
	Speed (km/h)	Departure time (s)	Waiting time (s)	F (£)	W (£)	TC (£)		Speed (km/h)	Departure time (s)	Waiting time (s)	F (£)	W (£)	TC (£)
(0,3)	10	0	0	17.67	24.20	41.87	(0,3)	10	0	0	17.67	31.68	49.35
(3,2)	10, 72[a]	11,000	0	14.69	11.94	26.63	(3,2)	75.34	14,400	3400	11.47	5.26	16.72
(2,1)	72	16427.8	0	6.75	3.30	10.05	(2,1)	75.34	16789.2	0	6.88	3.15	10.03
(1,0)	75.34	17927.8	0	11.47	5.26	16.72	(1,0)	75.34	18222.7	0	11.47	5.26	16.72
Total			50.58	44.70	95.28						47.49	45.35	92.84

[a] *Transient* region.

Table 4
Comparison of S_N and S_D in Example 3.

Arc	S_N						Arc	S_D					
	Speed (km/h)	Departure time (s)	Waiting time (s)	F (£)	W (£)	TC (£)		Speed (km/h)	Departure time (s)	Waiting time (s)	F (£)	W (£)	TC (£)
(0,1)	10, 75.34[a]	0	0	25.86	32.73	58.59	(0,2)	10, 106.02[a]	5070.96	5070.96	24.81	34.10	58.91
(1,2)	75.34	14877.8	Inf.	Inf.	Inf.	Inf.	(2,1)	75.34	15,500	0	6.88	3.15	10.03
(2,3)	75.34	16311.3	Inf.	Inf.	Inf.	Inf.	(1,3)	75.34	16933.5	0	13.37	6.13	19.50
(3,0)	75.34	18700.5	Inf.	Inf.	Inf.	Inf.	(3,0)	75.34	19719.7	0	6.88	3.15	10.03
Total											51.95	46.54	98.48

[a] *Transient* region.

Table 5
Comparison of S_N and S_D in Example 4.

Arc	S_N						Arc	S_D					
	Speed (km/h)	Departure time (s)	Waiting time (s)	*F* (£)	*D* (£)	*TC* (£)		Speed (km/h)	Departure time (s)	Waiting time (s)	*F* (£)	*D* (£)	*TC* (£)
(0,3)	10, 75.34[a]	13743.8	13743.8	7.54	4.41	11.94	(0,3)	75.34	14,400	14,400	6.88	3.15	10.03
(3,2)	75.34	15746.4	0	11.47	5.26	16.73	(3,2)	75.34	15833.5	0	11.47	5.26	16.72
(2,1)	75.34	18135.6	0	6.88	3.15	10.04	(2,1)	75.34	18222.7	0	6.88	3.15	10.03
(1,0)	75.34	19569.1	0	11.47	5.26	16.73	(1,0)	75.34	19656.2	0	11.47	5.26	16.72
Total				37.36	18.07	55.43					36.70	16.82	53.52

[a] *Transient* region.

Table 6
Comparison of the driver wage policies in Example 5.

Arc	S_D The driver is paid from the beginning of the time horizon						Arc	S_D The driver is paid from departure					
	Speed (km/h)	Departure time (s)	Waiting time (s)	*F* (£)	*W* (£)	*TC* (£)		Speed (km/h)	Departure time (s)	Waiting time (s)	*F* (£)	*W* (£)	*TC* (£)
(0,1)	97.5	7200	7200	13.64	19.89	33.53	(0,3)	75.34	8566.5	8566.5	6.88	3.15	10.03
(1,2)	97.5	9046.15	0.00	8.17	2.44	10.61	(3,2)	75.34	10,000	0	11.47	5.26	16.73
(2,3)	97.5	10153.8	0.00	13.59	4.07	17.66	(2,1)	75.34	12389.2	0	6.88	3.15	10.03
(3,0)	75.34	12000.00	0.00	6.88	3.15	10.03	(1,0)	75.34	13822.7	0	11.47	5.26	16.73
Total				42.28	29.55	71.83					36.70	16.82	53.52

Table 5 shows that when there are lower time window restrictions at the customers and the driver is paid from its departure time, there can be strategic post-service waiting time at the depot in both solutions S_N and S_D. In the S_N solution, the reason for delaying the vehicle's departure is to reduce the driver cost by avoiding pre-service wait at the customer node. In contrast, in S_D solution, there is another reason for delaying the vehicle's departure, which is the desire to avoid traveling in congestion, thereby reducing emissions cost.

From the four examples just presented, we conclude that ignoring traffic congestion can have detrimental consequences on the timing of deliveries. Congestion is likely to increase costs or even lead to an infeasible solution (which can be seen as a solution with infinite costs) when customer nodes have delivery time windows. This is because the planner does not incorporate strategic post-service wait times motivated by traffic congestion in the vehicle schedules. We show that these strategic wait times can occur either at the depot or at the customer nodes.

3.2. Impact of the driver wage policy

In this section we investigate the impact of the driver wage policy on the optimal TDPRP solution, namely whether the driver is paid from the beginning of the time horizon or from his departure time. In the example below, the length of the congestion period is equal to 7200 s.

Example 5: Impact of driver wage policy on wait time and routing

In this example we assume the following service time windows (in seconds) at customer nodes: $l_1 = l_2 = 9000$, $l_3 = 10{,}000$, $u_1 = 19{,}000$, $u_2 = 15{,}000$, $u_3 = 12{,}000$. The optimal solutions for the two driver wage policies are compared in Table 6.

Table 6 shows that the driver wage policy may affect the resulting route. When the driver is paid from the beginning of the time horizon, the optimal route is (0,1,2,3,0) and it is optimal to wait until the end of the congestion period. When the driver is paid from his departure time, it is optimal to postpone his departure until after the end of the congestion period but this requires a change of route to (0,3,2,1,0) in order to meet the delivery time windows.

In summary, we see that it is important to take the driver wage policy into account when optimizing the route and schedule of the vehicles. When the driver is paid from his departure time, he generally leaves the depot later than if he was paid from the beginning of the time horizon, but this delay has to be compensated by either a change of route or a speed increase.

4. An integer linear programming formulation for the TDPRP

This section presents a mathematical formulation for the TDPRP. The objective is to determine a set of routes for the K vehicles, all starting and ending at the depot, along with their speeds on each arc, and then departure times from each node so as to minimize a total cost function encompassing driver and emissions costs. The objective function is not linear in the speed values. To linearize it, we discretize the free-flow speed following an approach used by Bektaş and Laporte (2011). Let

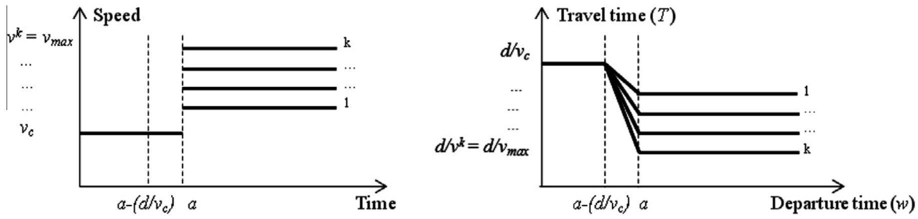

Fig. 4. Time-dependent speed and travel time profiles.

$R = \{1, \ldots, k\}$ be the index set of different speed levels and $v^1, \ldots, v^k$ denote the corresponding free-flow speeds where $v_c \leqslant v_{min} = v^1 < \cdots < v^k = v_{max}$. Fig. 4 illustrates the different speed values and corresponding travel time functions. Let $b^0 = 0$, $b^1 = (a - d/v_c)^+$, $b^2 = a$ and $b^3 = \infty$ and let $[b^{m-1}, b^m)$ denote the mth time interval, where $m \in \{1,2,3\}$. Specifically, $m = 1$ is the *all congestion* region, $m = 2$ is the *transient* region and $m = 3$ is the *all free-flow* region. We also define v^{mr} as the vehicle speed in time region m given free-flow speed v^r with $r \in R$, that is, $v^{1r} = v_c$, $v^{2r} = v_c$ and $v^{3r} = v^r$. These definitions allow us to rewrite (1) for arc (i,j) as $T(w, v_r) = \theta^{mr} w + \eta_{ij}^{mr}$, if $b^{m-1} \leqslant w < b^m$ and $r \in R$, where,

$$\theta^{mr} = \begin{cases} 0 & m = 1, 3 \\ \frac{v^{2r} - v^{3r}}{v^{3r}} & m = 2, \end{cases}$$

$$\eta_{ij}^{mr} = \begin{cases} \frac{d_{ij}}{v^{1r}} & m = 1 \\ \frac{d_{ij}}{v^{3r}} + \left(\frac{v^{3r} - v^{2r}}{v^{3r}}\right) a & m = 2 \\ \frac{d_{ij}}{v^{3r}} & m = 3. \end{cases}$$

The model uses the following decision variables:

x_{ij}	binary variable equal to 1 if a vehicle traverses arc $(i,j) \in A$, *0* otherwise,
z_{ij}^{mr}	binary variable equal to 1 if a vehicle traverses arc $(i,j) \in A$, leaving node i within time interval $m \in \{1,2,3\}$ with the free-flow speed v_r with $r \in R$, *0* otherwise,
f_{ij}	load carried on arc (i,j),
w_{ij}^{mr}	variable equal to the time instant at which a vehicle leaves node $i \in N$ to traverse arc (i,j) if within time interval $m \in \{1,2,3\}$ with the free-flow speed v_r with $r \in R$,
s_i	total time spent on a route that has node $i \in N_0$ as last visited before returning to the depot,
φ_i	time at which service at node $i \in N_0$ starts.

Given these variables, $\theta_{ij}^{mr} w_{ij}^{mr} + \eta_{ij}^{mr} x_{ij}^{mr}$ is equal to the travel time of a vehicle on arc $(i,j) \in A$ if the vehicle leaves node i within time interval $m \in \{1,2,3\}$ and uses free-flow speed v^r with $r \in R$.

We now present a mixed integer linear programming formulation for the TDPRP:

$$\text{Minimize} \quad \sum_{(i,j)\in A} \sum_{r\in R} \sum_{m=1}^{3} f_c \lambda k N_e V \left(\theta_{ij}^{mr} w_{ij}^{mr} + \eta_{ij}^{mr} z_{ij}^{mr}\right) \tag{5}$$

$$+ \sum_{(i,j)\in A} \sum_{r\in R} \sum_{m=1,3} f_c \lambda \gamma \beta (v^{mr})^3 \left(\theta_{ij}^{mr} w_{ij}^{mr} + \eta_{ij}^{mr} z_{ij}^{mr}\right) \tag{6}$$

$$+ \sum_{(ij)\in A} \sum_{r\in R} f_c \lambda \gamma \beta (v^{2r})^3 \left(a z_{ij}^{2r} - w_{ij}^{2r}\right) \tag{7}$$

$$+ \sum_{(i,j)\in A} \sum_{r\in R} f_c \lambda \gamma \beta (v^{3r})^3 \left(w_{ij}^{2r} + \theta_{ij}^{2r} w_{ij}^{2r} + \eta_{ij}^{2r} z_{ij}^{2r} - a z_{ij}^{2r}\right) \tag{8}$$

$$+ \sum_{(i,j)\in A} f_c \lambda \gamma \alpha_{ij} d_{ij} (\mu x_{ij} + f_{ij}) \tag{9}$$

$$+ \sum_{i\in N_0} d_c s_i \tag{10}$$

subject to

$$\sum_{j\in N_0} x_{0j} = K \tag{11}$$

$$\sum_{i\in N} x_{ij} = 1 \qquad \forall\ j \in N_0 \tag{12}$$

$$\sum_{j\in N} x_{ij} = 1 \qquad \forall\ i \in N_0 \tag{13}$$

$$\sum_{j\in N} f_{ji} - \sum_{j\in N} f_{ij} = q_i \qquad \forall\ i \in N_0 \tag{14}$$

$$q_j x_{ij} \leqslant f_{ij} \leqslant x_{ij}(Q - q_i) \qquad \forall\ (i,j) \in A \tag{15}$$

$$z_{ij}^{mr} b_{ij}^{m-1} \leqslant w_{ij}^{mr} \leqslant z_{ij}^{mr} b_{ij}^{m} \qquad \forall\ (i,j) \in A, m \in \{1,2,3\}, r \in R \tag{16}$$

$$\sum_{i\in N}\sum_{m=1}^{3}\sum_{r\in R}\left(w_{ij}^{mr} + \theta_{ij}^{mr} w_{ij}^{mr} + \eta_{ij}^{mr} z_{ij}^{mr}\right) \leqslant \varphi_j \qquad \forall\ j \in N_0 \tag{17}$$

$$\sum_{j\in N}\sum_{r\in R}\sum_{m=1}^{3} w_{ij}^{mr} \geqslant \varphi_i + h_i \qquad \forall\ i \in N_0 \tag{18}$$

$$l_i \leqslant \varphi_i \leqslant u_i \qquad \forall\ i \in N_0 \tag{19}$$

$$s_i \geqslant \sum_{r\in R}\sum_{m=1}^{3}\left(w_{i0}^{mr} + \theta_{i0}^{mr} w_{i0}^{mr} + \eta_{i0}^{mr} z_{i0}^{mr}\right) \qquad \forall\ i \in N_0 \tag{20}$$

$$\sum_{m=1}^{3}\sum_{r\in R} z_{ij}^{mr} = x_{ij} \qquad \forall\ (i,j) \in A \tag{21}$$

$$z_{ij}^{mr} \in \{0,1\} \qquad \forall\ (i,j) \in A, m \in \{1,2,3\}, r \in R \tag{22}$$

$$x_{ij} \in \{0,1\} \qquad \forall\ (i,j) \in A \tag{23}$$

$$f_{ij} \geqslant 0 \qquad \forall\ (i,j) \in A, m \in \{1,2,3\}, r \in R. \tag{24}$$

The first five parts of the objective function represent the cost of emissions. In particular, (5) computes the cost induced by the *engine module*, the terms (6)–(8) measure the cost induced by the *speed module*, and (9) is the cost induced by the *weight module*. More precisely, (6) calculates the emissions cost generated by the *speed module* in the *all congestion* and in the *all free-flow* regions, while (7) and (8) represent the emissions cost generated by the speed module in the *transient* region. Finally, the last term (10) measures the total driver wage when the driver is paid from the beginning of the time horizon. In contrast, if the driver was paid from its departure time, the total driver wage would be $\sum_{i\in N_0} d_c s_i - \sum_{j\in N_0}\sum_{r\in R}\sum_{m=1}^{3} d_c w_{0j}^{mr}$.

Constraint (11) indicates that exactly K vehicles depart from the depot. Constraints (12) and (13) guarantee that each customer is visited exactly once. Constraints (14) and (15) model the flow on each arc, and ensure that vehicle capacities are respected. The boundary conditions on the departure time are imposed by constraint (16). Constraints (17) and (18) are used to express the temporal relationship between arrival time and service time, and between service time and departure time, respectively. The time windows restrictions at customer nodes are imposed by constraint (19). Constraint (20) computes the time at which the vehicle returns to the depot. The relationship between speed and arc-traversal variables is expressed by constraint (21). Finally, constraints (22)–(24) enforce the integrality and nonnegativity restrictions on the variables.

We provide a numerical analysis of the performance of this formulation in Section 7.

5. Analytical results based on a single-arc network

We now consider a special case of the TDPRP on a network with two nodes, i.e., the depot and one customer node. The aim is to gain insights by analyzing this special case of the problem; as will be shown in Sections 6 and 7, the results obtained in this section are useful for optimizing the TDPRP on a fixed route and for improving the computational performance of the integer linear programming formulation.

We minimize the cost of going from the depot to the customer node (hence, ignoring the return trip to the depot). The customer node has a time window $[l,u]$. Service time at the customer node is equal to h (in this section it can be set equal to zero without loss of generality but we include it because it becomes a relevant variable for the problem presented in Section 6). We assume, without loss of generality, that the demand at the customer is equal to zero and that there is a two-level speed profile with an initial congestion period a, as described in Section 2.1.

In this special case there are only two decision variables: the departure time w from the depot and the free-flow speed v_f for the vehicle serving the customer. We must have $v_f \in [v_{min}, v_{max}]$ and $w \geqslant \epsilon$, where $\epsilon \geqslant 0$ is the earliest time at which the vehicle can leave the depot. For example ϵ can represent loading time at the depot. We refer to ϵ as the beginning of the planning horizon; $w - \epsilon$ is the (strategic) waiting time at the depot. Without loss of generality we assume that $a \geqslant \epsilon$ and $\epsilon \leqslant l \leqslant u \leqslant \infty$ (for example, if $a < \epsilon$, then the problem can be solved by setting $a = \epsilon$).

Our objective is to minimize the total cost function $TC(w, v_f)$ so that the arrival time at the customer node does not exceed u. In other words, the optimization problem is

$$\begin{aligned} &\underset{\substack{w \geqslant \epsilon \\ v_{min} \leqslant v_f \leqslant v_{max}}}{\text{minimize}} && TC(w, v_f) = f_c F(w, v_f) + d_c W(w, v_f) \\ &\text{subject to} && T(w, v_f) + w \leqslant u, \end{aligned}$$

where F and T are as defined in Section 2 and $W(w, v_f)$ denotes the time for which the driver is paid. If the driver is paid from the beginning of the time horizon (i.e., ϵ), then $W(w, v_f) = \max\{w - \epsilon + T(w, v_f), l - \epsilon\} + h$. If the driver is paid from his departure time (i.e., w), then $W(w, v_f) = \max\{T(w, v_f), l - w\} + h$.

For the single-arc problem to be feasible, the vehicle must be able to reach the customer node by time u if it does not wait at the depot, i.e. if $w = \epsilon$. By leaving immediately, the vehicle is either (i) in the *all congestion* region, i.e., when $\epsilon \leqslant a - d/v_c$, in which case $u \geqslant \epsilon + d/v_c$, or (ii) in the *transient* region, i.e., when $\epsilon \geqslant a - d/v_c$, in which case $u \geqslant a + (d - (a - \epsilon)v_c)/v_{max}$. We can summarize these two conditions as follows: $u \geqslant \min\{a, \epsilon + d/v_c\} + (d - (a - \epsilon)v_c)^+/v_{max}$. In what follows we assume that this condition is satisfied.

Let v_w^u be the free-flow speed required for the driver to arrive at the customer exactly at time u when leaving the depot at time w. Then

$$v_w^u = \begin{cases} \frac{d-(a-w)^+ v_c}{u-\max\{a,w\}}, & \text{if } w \in [\max\{\epsilon, a - d/v_c\}, u] \text{ and } u > a \\ \infty, & \text{otherwise.} \end{cases}$$

Similarly, let v_w^l be the free-flow speed required for the driver to arrive at the customer exactly at time l when leaving the depot at w. Then

$$v_w^l = \begin{cases} \frac{d-(a-w)^+ v_c}{l-\max\{a,w\}}, & \text{if } w \in [\max\{\epsilon, a - d/v_c\}, l] \text{ and } l > a \\ \infty, & \text{otherwise.} \end{cases}$$

The departure time w from the depot must be such that $v_w^u \leqslant v_{max}$ otherwise it is not possible to arrive by time u. Let w_{max}^u denote the time at which the vehicle needs to depart from the depot to reach the customer at exactly time u, driving at free-flow speed v_{max}.

$$w_{max}^u = \begin{cases} u - \frac{d}{v_{max}}, & \text{if } v_{max} \geqslant v_a^u \text{ and } u > a \\ a - \frac{d-(u-a)v_{max}}{v_c}, & \text{if } v_{max} < v_a^u \text{ and } u > a \\ u - \frac{d}{v_c} & \text{if } \epsilon \leqslant u \leqslant a. \end{cases}$$

In other words, w_{max}^u is an upper bound on the departure time, i.e., for a value of the departure time w to be feasible we need $w \in [\epsilon, w_{max}^u)$. Similarly let w_{max}^l be the maximum departure time such that the driver arrives exactly at time l driving at free-flow speed v_{max}:

$$w_{max}^l = \begin{cases} l - \frac{d}{v_{max}}, & \text{if } v_{max} \geqslant v_a^l \text{ and } l > a \\ a - \frac{d-(l-a)v_{max}}{v_c}, & \text{if } v_{max} < v_a^l \text{ and } l > a \\ l - \frac{d}{v_c} & \text{if } \epsilon \leqslant l \leqslant a. \end{cases}$$

We first determine the optimal free-flow speed v_f for a given departure time $w \in [\max\{\epsilon, a - d/v_c\}, w_{max}^u]$. As shown in Lemma 5.1, this can be done by comparing the speed levels v_w^l and v_w^u to two key speed levels: $\bar{v} = ((f_c \lambda k N_e V + d_c)/2 f_c \lambda \beta \gamma)^{1/3}$ and $\underline{v} = (kN_eV/2\beta\gamma)^{1/3}$. The speed level $\bar{v}$ minimizes emissions and driver costs, i.e., TC, in the absence of any time window, whereas the speed $\underline{v}$ minimizes emissions consumption only, i.e., F, in the absence of any time windows. Both values are independent of the departure time w. These speed values have previously been identified by Demir et al. (2012).

Lemma 5.1. *Consider a single-arc TDPRP instance and a departure time w such that $w \in [\max\{\epsilon, a - d/v_c\}, w_{max}^u]$. The optimal free-flow speed is $\min\{v_{max}, v^*\}$, where v^* is given as follows: (i) if $v_w^l \leqslant \underline{v}$ then v^* is $\max\{v_{min}, \underline{v}\}$, (ii) if $\underline{v} \leqslant v_w^l \leqslant \bar{v}$ then v^* is $\max\{v_{min}, v_w^l\}$, (iii) if $v_w^u \leqslant \bar{v} \leqslant v_w^l$ then v^* is $\max\{v_{min}, \bar{v}\}$, (iv) if $\bar{v} \leqslant v_w^u$ then v^* is $\max\{v_{min}, v_w^u\}$.*

Note that the optimal speed for a given departure time does not depend on the driver wage policy. Using Lemma 5.1, we can reduce the problem of minimizing TC to a unidimensional optimization problem, that is, we set w as the unique decision variable.

Observe that the minimum speed limitation only affects the optimal solution if $v_{min} > \underline{v}$.

We now provide the full characterization of the optimal solution for the special case where $v_{min} \leqslant \underline{v}$ (for the sake of conciseness)[1]. Let $S = (w^*, v_f^*)$ denote a solution, where w^* is the optimal departure time and v_f^* is the optimal free-flow speed, Theorem 5.1 provides the solution when the driver is paid from the beginning of the time horizon, i.e, from time ϵ, and Theorem 5.2 provides the solution when the driver is paid from his departure time i.e., from time w. Observe that whenever the vehicle

[1] For most practical purposes, it is reasonable to assume that the minimum speed limit is lower than the speed which minimizes emissions costs. A full characterization of the optimal solution is available upon request.

traverses the entire arc during the congestion period, the free-flow speed is never used but we may still write $S = \left(w^*, v_f^*\right)$, with v_f^* being equal to any positive value.

Theorem 5.1. *Consider a single-arc TDPRP instance. If the driver is paid from the beginning of the time horizon, the optimal solution depends mainly on the relative values of the nine speed levels:* v_{max}, $\underline{v}$, $\bar{v}$, $\hat{v} = \left((kN_eV + \beta\gamma v_c^3)/3\beta\gamma v_c\right)^{1/2}$, $\check{v} = \left((f_c\lambda kN_eV + d_c + f_c\lambda\beta\gamma v_{max}^3)/3f_c\lambda\beta\gamma v_{max}\right)^{1/2}$, v_ϵ^l, v_a^l, v_ϵ^u *and* v_a^u *and is given in Table A.11 in Appendix A.*

Theorem 5.1 suggests that, when the driver is paid from the beginning of the time horizon, there are four important free-flow speed values: $\bar{v}$, $\underline{v}$, $\hat{v}$ and $\check{v}$, which only depend on the values from Table 1. In particular, the first two values are defined as in Lemma 5.1, and the latter two are comparison parameters. The intuition is as follows. Delaying the departure of the driver has two effects: on the one hand, it may increase the driver cost as the driver is paid for a longer period of time; on the other hand, it may reduce the time spent driving in congestion, allowing the driver to reach a higher average driving speed and spend less time on the road. The engine module component of the emissions cost is decreasing in the departure time, whereas the driver cost and speed module are increasing in it. As a result, the overall impact on the total cost depends on the trade-off between these costs. More specifically, when $v_{max} \leqslant \bar{v}$ ($v_{max} > \bar{v}$), the total cost function is initially decreasing in the *transient* region (where both effects are active) only if $\hat{v} \geqslant \check{v}$($\hat{v} \geqslant \bar{v}$). In this case, it may be beneficial to postpone the departure time past time ϵ because the drop in the engine module part of the emissions cost more than offsets the increase in driver cost and speed module.

Beside the speeds just described, the optimal solution also depends on other four free-flow speed values: v_ϵ^l, v_ϵ^u, v_a^l, and v_a^u, which only depend on the instance parameters, that is, l, u, d and a.

Theorem 5.2. *Consider a single-arc TDPRP instance. If the driver is paid from his departure time, the optimal solution depends mainly on the relative values of the eight speed levels:* v_{max}, $\underline{v}$, $\bar{v}$, $\tilde{v} = \left((f_c\lambda kN_eV + d_c + f_c\lambda\beta\gamma v_c^3)/3f_c\lambda\beta\gamma v_c\right)^{1/2}$, v_ϵ^l, v_a^l, v_ϵ^u *and* v_a^u *and is given in Table A.12 in Appendix A.*

When the driver is paid from his departure time, delaying departure does not lead to an increase in the driver cost. In fact it may lead to a decrease since waiting may mean less driving in congestion and therefore spending less time on the road. In this case the trade-off is between the speed module of the emissions cost, which is increasing in the departure time, and the driver cost and engine module which are decreasing.

We make the following remarks about the optimal solutions under both driver wage policies.

Remark 5.1. Consider a single-arc TDPRP instance.

- If there is no time window, i.e. $l = 0$ and $u = \infty$, and the driver is paid from the beginning of the time horizon, then one of the following two solutions is optimal: either leave the depot immediately ($w^* = \epsilon$), or wait until the end of the congestion period ($w^* = a$). In both cases the optimal speed is $\bar{v}$. Alternatively, when the driver is paid from his departure time, leaving the depot at the end of the congestion period ($w^* = a$) and driving at free-flow speed $\bar{v}$ is optimal.
- When the driver is paid from the beginning of the time horizon, there always exists an optimal solution where the driver leaves at or before the end of the congestion period, i.e., at time $w^* \leqslant a$. However, when the driver is paid from his departure time, it may be optimal to leave the depot after the end of the congestion period, i.e., at time $w^* > a$.
- The optimal departure time when the driver is paid from the beginning of the time horizon is at most equal to the optimal departure time when the driver is paid from his departure time. This is due to the fact that there is an extra incentive to delay departure when the driver is paid from his departure time, which is to reduce the driver cost.
- If there is no congestion period, the TDPRP reduces to the PRP. In this case, our results show that, when the driver is paid from the beginning of the time horizon, there always exists an optimal solution where the driver leaves the depot immediately, i.e., $w^* = \epsilon$. However, this result is not true when the driver is paid from his departure time. In this case, even in the absence of congestion, it may be optimal to delay the departure of the vehicle in order to save on the driver cost, when leaving at time ϵ would lead to a pre-service waiting time at the customer node.
- The results of this section also apply to the case where emissions costs are ignored (i.e., if f_c is set to 0) so that the objective function reduces to minimizing only the driver cost, that is, Theorems 5.1 and 5.2 can be used to obtain an optimal solution (note that $\bar{v} = \check{v} = \tilde{v} = \infty$ in this case). When the driver is paid from the beginning of the time horizon, it is always optimal for him to leave immediately and drive at speed v_{max}. However, when the driver is paid from his departure time, it may be optimal to wait at the depot.

The following theorem establishes the relationship between the optimal departure time and the time window $[l,u]$.

Theorem 5.3. *The (earliest) optimal departure time from the depot w^* is non-decreasing in l and u. The optimal free-flow speed v^* (whenever it is used) is non-increasing in l and u.*

The following example illustrates how the optimal solution to the TDPRP varies with l and u.

Table 7
Optimal solution $S = \left(w^*, v_f^*\right)$ as a function of lower and upper time window.

l	u	Driver paid from the beginning of the time horizon			Driver paid from departure time		
		w^*	v_f^*	Arrival time	w^*	v_f^*	Arrival time
7500	11,545	0	110 (v_m)	11,545 (u)	0	110 (v_m)	11,545 (u)
7500	12,000	0	85 (v_ϵ^u)	12,000 (u)	2631.58 (<a)	110 (v_m)	12,000 (u)
7500	13,000	3301.98 (<a)	77.58 ($\hat{v}$)	13,000 (u)	8421.05 (<a)	110 (v_m)	13,000 (u)
7500	14,700	10,000 (a)	76.60 (v_a^u)	14,700 (u)	10,000 (a)	76.60 (v_u^a)	14,700 (u)
7500	70,000	10,000 (a)	75.34 ($\bar{v}$)	14778.20 ($\in(l,u)$)	10,000 (a)	75.34 ($\bar{v}$)	14778.20 ($\in(l,u)$)
15,000	70,000	10,000 (a)	72 (v_a^l)	15,000 (l)	10221.79 (>a)	75.34 ($\bar{v}$)	15,000 (l)
25,000	70,000	10,000 (a)	55.19 ($\underline{v}$)	16,523 (<l)	20221.79 (>a)	75.34 ($\bar{v}$)	25,000 (l)

Example 5.1. The parameters in Table 1 imply that $\underline{v}$ = 55.19 km/h and $\bar{v} = 75.34$ km/h. Let ϵ = 0, d = 100 km, v_c = 19 km/h, v_{min} = 50 km/h, v_m = 110 km/h and a = 10,000 s. This implies that $\hat{v} = 77.58$ km/h and $\tilde{v} = 122.99$ km/h. Table 7 shows the optimal solution as a function of the lower (l) and upper (u) time windows, given in seconds.

We see that for low values of l and u, it is optimal for the driver to leave the depot immediately and arrive at the customer node exactly at time u. As u increases, it becomes optimal to wait at the depot and eventually arrive between l and u. Then as l is increased, the optimal arrival time becomes exactly l and then possibly (when the driver is paid from the beginning of the time horizon) a value less than l, meaning that there is a pre-service waiting time.

Based on the properties of single-arc TDPRP instance we derive the following results which also apply to the general case.

Lemma 5.2. *Given a TDPRP instance,*

(i) *it is never optimal for drivers to drive at a free-flow speed lower than* $\underline{v}$*;*
(ii) *if drivers are paid from their departure time, it is never optimal for them to drive on the first arc of a route at a free-flow speed lower than* $\min\{\bar{v}, v_{max}\}$.

These results will be useful to improve the efficiency of the MIP formulation, as discussed in Section 7.

6. Departure time and speed optimization on fixed routes

In this section, we consider a special case of the TDPRP where there is only one vehicle and a fixed sequence in which the customer nodes are to be visited. We refer to this problem as the Departure Time and Speed Optimization Problem (DSOP). Let $(0, \ldots, n+1)$ be the fixed sequence of nodes. Node $n+1$ may be a copy of the depot, implying a return to the origin but this does not have to be the case. Let d_i denote the distance on arc $(i, i+1)$ with $0 \leqslant i \leqslant n$. As described in Section 2, l_i, u_i and h_i are respectively the lower time window limit, the upper time window limit and the service time at node i. Without loss of generality the demand values at each nodes are set equal to zero. We assume the driver is paid from the beginning of the time horizon.

The decision variables are (i) the departure time from node i, denoted w_i for $i = 0, \ldots, n$ and (ii) the free-flow speed driven on arc $(i, i+1)$ (if possible), denoted v_i for $i = 0, \ldots, n$. We must have $v_i \in [v_{min}, v_{max}]$ for $i = 0, \ldots, n$, $w_0 \geqslant \epsilon$, where ϵ denotes the earliest time the driver can leave the depot, and $w_i \geqslant \max\{l_i, w_{i-1} + T_{i-1}(w_{i-1}, v_{i-1})\} + h_i$ for $i = 1, \ldots, n$, where $T_{i-1}(w_{i-1}, v_{i-1})$ denotes the travel time of the vehicle between nodes $i-1$ and i.

Solution methods for the DSOP. The TDPRP reduces to K instances of the DSOP if the route of each of the K vehicles is fixed. This means that, given a discrete set of free flow speeds, the DSOP can, in principle, be solved by a commercial optimization software using the MIP model presented in Section 4, where constraints (11)–(15), (23), (and) (24) are relaxed. Even in this case, however, solving the resulting problem requires considerable computational effort due to the large number of binary decision variables and the precision of the solution depends on the level of discretization of the free-flow speeds. To overcome these limitations, we propose a polynomial time solution method which, in our numerical experiments, has been observed to solve the problem to optimality in every case we have considered. Our DSOP algorithm builds on the solution to the Speed Optimization Problem (SOP) proposed by Norstad et al. (2010) and Hvattum et al. (2013) for ship routing, which was then adapted to the PRP by Demir et al. (2012). These authors propose an algorithm to compute the optimal solution by recursively adjusting the travel speed for segments of the route until a feasible solution is found. Their method optimizes the travel speed only and is exact provided the total cost function is convex (Hvattum et al., 2013). In contrast, our algorithm is more general because it optimizes two sets of decision variables, namely the departure times and free flow speeds and the total cost function is no longer convex. As a consequence, the solution methods proposed for the SOP cannot be used to solve the DSOP. Our proposed method builds on the analytical properties presented in Section 5 and maintains the recursive nature of the algorithm proposed for the SOP.

In this paper, we provide a brief description of our DSOP algorithm as well as the pseudo-code in Appendix B. For more details about the algorithm we refer to Franceschetti et al. (2013). A solution to the DSOP problem is obtained by setting $s = 0$ and $e = n+1$. The DSOP algorithm operates as follows. It first solves a *relaxed* problem without any time windows at intermediary nodes, that is, with only the time window at the end node maintained. This solution is calculated by reducing the problem to a single-arc TDPRP which is solved using Theorem 5.1. Once the solution to the relaxed problem has been calculated, the algorithm checks whether there are any time window violations at intermediate nodes, i.e., whether the arrival time at node i is lower than l_i or higher than u_i. In case of multiple violations, the algorithm selects the node p with the largest violation. The solution is calculated by calling the algorithm recursively on each side of node p, that is, by calling the function for $(s, \ldots, p)$ and for $(p, \ldots, e)$ separately.

7. Computational results

This section presents the results of computational experiments using the integer linear programming formulation of the TDPRP presented in Secion 4 and the DSOP algorithm discussed in Section 6. All tests were carried out using three sets of instances from the PRPLIB (http://www.apollo.management.soton.ac.uk/prplib.htm), with respectively 10, 15 and 20 nodes as described by Demir et al. (2012). All experiments were conducted by using CPLEX 12.1 on a server with 2.93 GHz and 1.1 Gb RAM. The nodes in these instances represent randomly selected cities from the United Kingdom, with real distances. The time windows and service times, however, are randomly generated.

We set CPLEX to run sequentially in deterministic mode in a single thread. A common time-limit of three hours was imposed on all instances. To improve the efficiency of the formulation, we have used preprocessing to reduce the input data space by using the results of Lemma 5.2. More specifically, we downsize the set of free-flow speed levels R by setting $v^1 = \max\{v_{min}, \underline{v}\}$. We also include the values of the three speed levels $\bar{v}$, $\hat{v}$ and $\tilde{v}$ in the set of free-flow speed levels R, whenever these do not exceed the upper speed limit v_{max}. Finally, we supplement the formulation with two-node subtour breaking constraints $x_{ij} + x_{ji} \leq 1$, $\forall i,j \in N_0$, $i \neq j$, as was also done by Bektaş and Laporte (2011).

7.1. Performance on PRP instances

This section compares the performance of the proposed formulation for the TDPRP with that of Bektaş and Laporte (2011) for cases where there is no congestion. Table D.25 in Appendix D. presents the results of this experiment using 10-node instances. The first two columns of the table are self-explanatory, whereas the columns PRP and TDPRP present the total cost produced by the respective formulations and t (PRP) and t (TDPRP) present the associated computational times (in s) required to solve each instance to optimality. Compared with the mathematical formulation proposed by Bektaş and Laporte (2011), the TDPRP formulation is superior in terms of the computational time required to reach optimality. The average solution time with the new formulation is indeed significantly reduced from 508.47 to 5.52 s. The proposed model also can solve some larger PRP instances to optimality, in particular the 15- and 20-node instances, as shown Section in 7.3. The Bektaş and Laporte (2011) formulation could not handle such sizes because of the computational time requirements. One possible explanation for our formulation to be faster, despite being more general, is that it does not include any big-M parameters. Bektaş and Laporte (2011) use such a parameter both in the time window constraints and in the calculation of the total travel time.

7.2. Performance of the DSOP algorithm

We have performed several computational experiments in order to evaluate the performance of our DSOP algorithm. We compare the solutions obtained by our DSOP algorithm (denoted S_A) with the value obtained with the MIP formulation (denoted S_{IP}). The tests were run on three sets of instances from the PRPLIB. For each set of instances, the time window limits were relaxed by a factor δ, i.e. $l'_i = l_i - \delta(u_i - l_i)$ and $u'_i = u_i + \delta(u_i - l_i)$. In order to solve the MIP formulation, three sets (5, 10, and 15) of free-flow speed levels were considered. The results are reported in Table 8 which contains the average percentage deviation Dev (%) in total costs between S_A and S_{IP}, which is calculated as $100(TC(S_A) - TC(S_{IP}))/TC(S_A)$, where $TC(S)$ denotes the total cost of a solution S.

Table 8 shows that in all cases, the deviations are negative, implying that the solution computed with our DSOP algorithm is better than the solution obtained with CPLEX, i.e., $TC(S_{IP}) > TC(S_A)$. This is because the MIP model optimizes the free-flow speed over a finite set of 15 speed levels, whereas our algorithm considers speed as a continuous variable. These findings are consistent with our DSOP algorithm reaching the optimal solution in all the problem instances we considered.

7.3. Importance of modeling traffic congestion and impact of driver wage policy

In this section, we compare the results of cases with and without congestion, as we did in Section 3, using 10-, 15- and 20-node PRP instances. More specifically, by using the integer linear programming formulation described in Section 4, we compute a *time-dependent* optimal solution S_D. Using the same formulation and fixing the congestion period to zero, we compute a *time-independent* optimal solution S_N. We note that solving the problem by means of a *time-independent* approach may generate multiple optimal solutions which yield different total costs under a congestion scenario, in which case we select the solution with the minimum waiting time at the depot. For every instance, we assume the same two-level speed profile as defined in Section 2.1, and we consider both driver wage policies. The congestion speed v_c is set to 10 km/h and we consider two values for the length of the congestion period: 3600 and 7200 s. A summary of the results is provided in Tables 9 and 10

Table 8
Average *Dev* (%) for three sets of instances.

Instances	δ	a (s)	v_c (km/h)	Average *Dev* (%)
UK10	0.2	0	–	−0.005
UK10	0.3	3000	15	−0.005
UK10	0.5	3600	10	−0.002
UK15	0.7	3000	15	−0.004
UK20	1.0	3000	15	−0.008

Table 9
Summarized results for three sets of instances with an initial congestion period of 3600 s.

Instances	Drivers paid from the beginning of the time horizon					Drivers paid from departure				
	Infeasible S_N (%)	Infeasible S_D (%)	$t(S_N)$ (s)	$t(S_D)$ (s)	Saving (%)	Infeasible S_N (%)	Infeasible S_D (%)	$t(S_N)$ (s)	$t(S_D)$ (s)	Saving (%)
UK_10	30	0	3.663	4.981	3.206	30	0	3.136	4.561	6.330
UK_15	55	5	976.610	467.797	3.478	45	5	1148.129	668.824	5.705
UK_20[a]	19	0	1527.273	1119.881	2.937	24	0	2179.146	1003.909	5.736

[a] Results calculated only on the instances solved to optimality.

Table 10
Summarized results for three sets of instances with an initial congestion period of 7200 s.

Instances	Drivers paid from the beginning of the time horizon					Drivers paid from departure				
	Infeasible S_N (%)	Infeasible S_D (%)	$t(S_N)$ (s)	$t(S_D)$ (s)	Saving (%)	Infeasible S_D (%)	Infeasible S_D (%)	$t(S_N)$ (s)	$t(S_D)$ (s)	Saving (%)
UK_10	50	0	3.663	10.870	4.942	50	0	3.136	8.514	15.276
UK_15	80	10	976.610	463.724	5.055	85	10	1148.129	714.044	14.986
UK_20[a]	80	0	1527.273	3388.063	5.310	88	0	2179.146	3628.597	14.910

[a] Results calculated only on the instances solved to optimality.

(the full results over 60 instances are reported in Tables D.26–D.31 in Appendix D). These tables report, for each set of instances the percentage of infeasible solutions S_D and S_N, the average computational time (denoted by $t(S_N)$ and $t(S_D)$) and the average saving of using a *time-dependent* formulation. The latter is calculated as Saving % = $100(TC(S_N) - TC(S_D))/TC(S_N)$, representing the percentage decrease in costs which results from incorporating traffic congestion into planning vehicles routes and schedules.

Tables 9 and 10 show that in the presence of traffic congestion, using a *time-dependent* formulation significantly decreases the percentage of infeasible solutions. Furthermore the results also suggest that if both solutions are feasible, the *time-dependent* one can yield considerable cost savings over the *time-independent* one. The potential cost reduction increases proportionally to the length of the congestion period and can more than double when the driver is paid from his departure time. These implications support the assertions made in Section 3 by means of simple examples.

8. Conclusions

We have introduced and analyzed the time-dependent vehicle routing problem with time windows, which considers vehicles traveling under two subsequent periods of congestion and free-flow, respectively, and explicitly accounts for vehicle emissions which increases sharply when vehicles travel at slow speed. The modeling approach adopted in this paper yields solution with reduced greenhouse gas emissions. We emphasize that our results also hold for the time-dependent VRP even if emissions are not considered in the objective function.

We have provided an integer linear programming formulation, which is also valid for the special case of the problem where there is no congestion (e.g., as in the PRP introduced by Bektaş and Laporte (2011)). We have presented several examples that motivate idle waiting time, either pre- or post-service, at customer nodes or at the depot, in order to minimize a total cost function incorporating emissions and driver wages. We have derived a complete characterization of the optimal solution for a single-arc version of the TDPRP, identifying conditions under which it is optimal to wait before departure, and the associated amount of time. The characterization prescribes optimal speed levels under various conditions associated with time windows, the length of the congestion period and the speed limits. The analytical results derived in the paper were used to strengthen the computational performance of the mathematical formulation. Computational results have confirmed that the proposed formulation computationally outperforms the formulation recently proposed for the PRP. Moreover, the analytical expressions for optimal speeds can easily be used as a "rule-of-thumb" for the design of vehicle routes under congestion.

The paper has also described a procedure to optimize departure times and speeds on a fixed route, also building on the analytical results proven for the single-arc version of the problem. The procedure extends previous algorithms specifically designed for the speed-optimization problem (e.g., Norstad et al., 2010; Hvattum et al., 2013; Demir et al., 2012). The combined departure time and speed optimization problem is significantly more complicated. The pseudocode we have proposed for its solution was empirically shown to run very quickly and consistently provide highly accurate solutions on realistic instances. Our procedure can be embedded within algorithms for the TDPRP, or can be used as a stand-alone routine when vehicle routes have already been fixed. One obvious extension of the paper is to study the problem with multiple time zones where there are multiple occurrences of congestion and free-flow traffic conditions. The most likely case to arise in practice is a four-period problem corresponding to morning congestion, followed by a period free-flow, and a repetition of this pattern in afternoon rush-hour and evening traffic. Our study indicates that this extension is likely to be significantly more complicated to analyze, but our work can serve as a good starting point for its analysis.

Acknowledgements

The work was partly supported by the Dutch Institute for Advanced Logistics under the project 4C4D and by the Canadian Natural Sciences and Engineering Research Council under Grant 39682-10. This support is gratefully acknowledged. Thanks are due to the referees for their valuable comments.

Appendix A. Optimal solution tables

Tables A.11 and A.12.

Appendix B. Pseudocode for the DSOP procedure

Algorithm 1. DSOP algorithm part 1

function $\left[w_s^*,\ldots,w_{e-1}^*, v_s^*,\ldots,v_{e-1}^*\right] = \text{DSOP } s, e, \epsilon_s, a$
  $[r, w_s, \ldots, w_{e-1}, v_s, \ldots, v_{e-1}] \leftarrow \text{SOLVE\_RELAXED } (s, e, \epsilon_s, a)$;
  $violation \leftarrow 0$, $p \leftarrow 0$;
  for $i \leftarrow r+1$ to $e-1$ **do**
    $g_i \leftarrow \max\{0, l_i - w_{i-1} - T_{i-1}(w_{i-1}, v_{i-1}), w_{i-1} + T_{i-1}(w_{i-1}, v_{i-1}) - u_i\}$;
    if $g_i \geqslant violation$ **then**
      $violation \leftarrow g_i$, $p \leftarrow i$;
    end if
  end for
  if $violation > 0$ and $w_{p-1} + T_{p-1}(w_{p-1}, v_{p-1}) < l_p$ **then**
    $u_p \leftarrow l_p$;
    $\left[w_s^*,\ldots,w_{p-1}^*, v_s^*,\ldots,v_{p-1}^*\right] \leftarrow \text{DSOP } (s, p, \epsilon_s, a)$;
    $\epsilon_p \leftarrow \max\left\{w_{p-1}^* + T_{p-1}\left(w_{p-1}^*, v_{p-1}^*\right), l_p\right\} + h_p$;
    $\tilde{a}_p \leftarrow \max\{\epsilon_p, a\}$;
    $\left[w_p^*,\ldots,w_{e-1}^*, v_p^*,\ldots,v_{e-1}^*\right] \leftarrow \text{DSOP } (p, e, \epsilon_p, \tilde{a}_p)$;
  end if
  if $violation > 0$ and $w_{p-1} + T_{p-1}(w_{p-1}, v_{p-1}) > u_p$ **then**
    $l_p \leftarrow u_p$;
    $\left[w_s^*,\ldots,w_{p-1}^*, v_s^*,\ldots,v_{p-1}^*\right] \leftarrow \text{DSOP } (s, p, \epsilon_s, a)$;
    $\epsilon_p \leftarrow \max\left\{w_{p-1}^* + T_{p-1}\left(w_{p-1}^*, v_{p-1}^*\right), l_p\right\} + h_p$;
    $\tilde{a}_p \leftarrow \max\{\epsilon, a\}$;
    $\left[w_p^*,\ldots,w_{e-1}^*, v_p^*,\ldots,v_{e-1}^*\right] \leftarrow \text{DSOP } (p, e, \epsilon_p, \tilde{a}_p)$;
  end if
end function

The DSOP algorithm also uses as inputs the problem parameters (v_c, v_{max}, d_i for $i = s, \ldots, e-1$, l_j, u_j, h_j for $j = s, \ldots, e$) but for the sake of conciseness, these are not written as variables in the function declaration.

Algorithm 2. DSOP algorithm part 2

function $[r, w_s^*, \ldots, w_{e-1}^*, v_s^*, \ldots, v_{e-1}^*] =$ SOLVE_RELAXED s, e, ϵ_s, a
  for $i \leftarrow s$ to $e-1$ **do**
    $\underline{t}_i \leftarrow a - \epsilon_s - \sum_{j=s+1}^{i} h_j - \sum_{j=s}^{i} d_j/v_c, \bar{t}_i \leftarrow a - \epsilon_s - \sum_{j=s+1}^{k} h_j - \sum_{i=s}^{i-1} d_j/v_c$;
  end for
  $\hat{k} \leftarrow s$;
  while $\hat{k} < e-1$ and $\bar{t}_{\hat{k}+1} > 0$ **do**
    $\hat{k}++$;
  end while
  $i \leftarrow s$, $\epsilon_i \leftarrow \epsilon_s$, $K = \emptyset$;
  while $i \leqslant \hat{k}$ **do**
    $\tilde{d}_i \leftarrow \sum_{j=i}^{e-1} d_j, \tilde{a}_i \leftarrow \max\{\epsilon_i, a\}, \tilde{h}_i \leftarrow \sum_{j=i+1}^{e-1} h_j, \tilde{u}_i \leftarrow u_e - \tilde{h}_i, \tilde{l}_i \leftarrow l_e - \tilde{h}_i$;
    $(\tilde{w}_i, \tilde{v}_i) \leftarrow$ SINGLE_ARC_TDPRP $(\tilde{a}_i, v_c, v_{max}, \tilde{d}_i, \epsilon_i, \tilde{l}_i, \tilde{u}_i)$; ▹ use Theorem 5.1
    if $\tilde{a}_i - d_i/v_c \leqslant \tilde{w}_i \leqslant \tilde{a}_i$ **then**
      $c_i \leftarrow TC_{s,e}(\tilde{w}_i, \tilde{v}_i; \epsilon_s)$; ▹ use Eq. B.1
      $K \leftarrow K \cup \{i\}$;
    end if
    $i \leftarrow i+1$;
    $\epsilon_i \leftarrow \epsilon_{i-1} + d_{i-1}/v_c + h_i$;
  end while
  $r \leftarrow \arg\min_{i \in K} c_i$;
  if $\underline{t}_{e-1} > 0$ and $c_r > TC_{s,\,e}(\epsilon_{e-1}, v_c; \epsilon_s)$ **then**
    $r \leftarrow e, v_r^* \leftarrow v_c$;
  else if $\underline{t}_{\hat{k}} \leqslant 0$ and $c_r > TC_{s,e}(\epsilon_{\hat{k}}, \tilde{v}_{\hat{k}}; \epsilon_s)$ **then**
    $r \leftarrow \hat{k}, w_r^* \leftarrow \epsilon_{\hat{k}}, v_r^* \leftarrow \tilde{v}_{\hat{k}}$;
  else if $\underline{t}_{\hat{k}} > 0$ **then**
    $\epsilon_{\hat{k}+1} \leftarrow \epsilon_{\hat{k}} + d_{\hat{k}}/v_c + h_{\hat{k}+1}, \tilde{d}_{\hat{k}+1} \leftarrow \sum_{j=\hat{k}+1}^{e-1} d_j, \tilde{a}_{k+1} \leftarrow \max\{\epsilon_{\hat{k}+1}, a\}$;
    $\tilde{h}_{\hat{k}+1} \leftarrow \sum_{j=\hat{k}+1}^{e-1} h_j, \tilde{u}_{\hat{k}+1} \leftarrow u_e - \tilde{h}_{\hat{k}+1}, \tilde{l}_{k\hat{+}1} \leftarrow l_e - \tilde{h}_{\hat{k}+1}$;
    $(\tilde{w}_{\hat{k}+1}, \tilde{v}_{\hat{k}+1}) \leftarrow$ SINGLE_ARC_TDPRP $(\tilde{a}_{\hat{k}+1}, v_c, v_{max}, \tilde{d}_{\hat{k}+1}, \epsilon_{\hat{k}+1}, \tilde{l}_{\hat{k}+1}, \tilde{u}_{\hat{k}+1})$;
    if $c_r > TC_{s,e}(\epsilon_{\hat{k}+1}, \tilde{v}_{\hat{k}+1}; \epsilon_s)$ **then**
      $r \leftarrow \hat{k}+1, w_r^* \leftarrow \epsilon_{\hat{k}+1}, v_r^* \leftarrow \tilde{v}_{\hat{k}+1}$;
  end if
  end if
  for $i \leftarrow s$ to $r-1$ **then**
    $w_i^* \leftarrow \epsilon_i \; v_i^* \leftarrow v_c$;
  end for
  for $i \leftarrow r+1$ to $e-1$ **do**
    $w_i^* \leftarrow a + (d_r - (a - w_r)v_c)/v_r + \sum_{j=r+1}^{i-1} d_j/v_c + \sum_{j=r+1}^{i} h_j, v_i^* \leftarrow v_r^*$;
  end for
end function

The function SOLVE_RELAXED (s, e, ϵ_s) calculates the optimal departure times, i.e. $w_s, \ldots, w_{e-1}$, and free flow speeds, i.e., $v_s, \ldots, v_{e-1}$, between nodes s and e assuming that the earliest departure time from node s is ϵ_s and that time windows at nodes $s, \ldots, e-1$ are relaxed, i.e. that $l_s = \cdots = l_{e-1} = 0$ and $u_s = \cdots = u_{e-1} = \infty$. Only the time window at node e is maintained. Let

Table A.11
Optimal solution when driver is paid from the beginning of the time horizon.

Condition 1	Condition 2	Condition 3	Condition 4	Condition 5	Solution
$l \leqslant u \leqslant a$					(w, v_f) where $w \in \left[\epsilon, \max\left\{\epsilon, \left(l - \frac{d}{v_c}\right)\right\}\right]$
$l < a < u$	$v_{max} \leqslant \bar{v}$	$v_a^u \leqslant v_{max}$	$\hat{v} \geqslant \check{v}$		(a, v_{max}) or (ϵ, v_{max})
			$\hat{v} \leqslant \check{v}$		(ϵ, v_{max})
		$v_a^u \geqslant v_{max}$	$\hat{v} \geqslant \check{v}$		(w_{max}^u, v_{max}) or (ϵ, v_{max})
			$\hat{v} \leqslant \check{v}$		(ϵ, v_{max})
	$v_{max} \geqslant \bar{v}$	$v_a^u \leqslant \bar{v}$	$\hat{v} \geqslant \bar{v}$		$(a, \bar{v})$ or $(\epsilon, \bar{v})$
			$\hat{v} \leqslant \bar{v}$		$(\epsilon, \bar{v})$
		$\bar{v} \leqslant v_a^u \leqslant v_{max}$	$\hat{v} \leqslant \bar{v}$	$v_\epsilon^u \leqslant \bar{v}$	$(\epsilon, \bar{v})$
				$v_\epsilon^u \geqslant \bar{v}$	(ϵ, v_ϵ^u)
			$\bar{v} \leqslant \hat{v} \leqslant v_a^u$	$v_\epsilon^u \leqslant \hat{v}$	$(\hat{w}^u, \hat{v})$ or $(\epsilon, \bar{v})$
				$v_\epsilon^u \geqslant \hat{v}$	(ϵ, v_ϵ^u)
			$\hat{v} \geqslant v_a^u$		(a, v_u^a) or $(\epsilon, \bar{v})$
		$v_a^u \geqslant v_{max}$	$\hat{v} \leqslant \bar{v}$	$v_\epsilon^u \leqslant \bar{v}$	$(\epsilon, \bar{v})$
				$v_\epsilon^u \geqslant \bar{v}$	(ϵ, v_ϵ^u)
			$\bar{v} \leqslant \hat{v} \leqslant v_{max}$	$v_\epsilon^u \leqslant \hat{v}$	$(\hat{w}^u, \hat{v})$ or $(\epsilon, \bar{v})$
				$v_\epsilon^u \geqslant \hat{v}$	(ϵ, v_ϵ^u)
			$\hat{v} \geqslant v_{max}$		(w_{max}^u, v_{max}) or $(\epsilon, \bar{v})$
$a < l < u$	$v_{max} \leqslant \underline{v}$	$v_a^l \leqslant v_{max}$			(w, v_{max}) where $w \in [a, w_{max}^l]$
		$v_a^u \leqslant v_{max} \leqslant v_a^l$	$\hat{v} \geqslant \check{v}$		(a, v_{max})
			$\hat{v} \leqslant \check{v}$		(w_{max}^l, v_{max})
		$v_a^u \geqslant v_{max}$	$\hat{v} \geqslant \check{v}$		(w_{max}^u, v_{max})
			$\hat{v} \leqslant \check{v}$		(w_{max}^l, v_{max})
	$\underline{v} \leqslant v_{max} \leqslant \bar{v}$	$v_a^l \leqslant \underline{v}$			$(w, \underline{v})$ where $w \in [a, \underline{w}^l]$
		$\underline{v} \leqslant v_a^l \leqslant v_{max}$	$v_a^l \geqslant \hat{v}$	$v_\epsilon^l \leqslant \hat{v}$	$(\hat{w}^l, \hat{v})$
				$v_\epsilon^l \geqslant \hat{v}$	(ϵ, v_ϵ^l)
			$v_a^l \leqslant \hat{v}$		(a, v_a^l)
		$v_a^u \leqslant v_{max} \leqslant v_a^l$	$\hat{v} \leqslant v_{max}$	$v_\epsilon^l \leqslant \hat{v}$	$(\hat{w}^l, \hat{v})$
				$\hat{v} \leqslant v_\epsilon^l \leqslant v_{max}$	(ϵ, v_ϵ^l)
				$v_\epsilon^l \geqslant v_{max}$	(ϵ, v_{max})
			$v_{max} \leqslant \hat{v} \leqslant \check{v}$	$v_\epsilon^l \leqslant v_{max}$	(w_{max}^l, v_{max})
				$v_\epsilon^l \geqslant v_{max}$	(ϵ, v_{max})
			$\hat{v} \geqslant \check{v}$		(a, v_{max})
		$v_a^u \geqslant v_{max}$	$\hat{v} \leqslant v_{max}$	$v_\epsilon^l \leqslant \hat{v}$	$(\hat{w}^l, \hat{v})$
				$\hat{v} \leqslant v_\epsilon^l \leqslant v_{max}$	(ϵ, v_ϵ^l)
				$v_\epsilon^l \geqslant v_{max}$	(ϵ, v_{max})
			$v_{max} \leqslant \hat{v} \leqslant \check{v}$	$v_\epsilon^l \leqslant v_{max}$	(w_{max}^l, v_{max})
				$v_\epsilon^l \geqslant v_{max}$	(ϵ, v_{max})
			$\hat{v} \geqslant \check{v}$		(w_{max}^u, v_{max})
	$v_{max} \geqslant \bar{v}$	$v_a^l \leqslant \underline{v}$			$(w, \underline{v})$ where $w \in [a, \underline{w}^l]$
		$\underline{v} \leqslant v_a^l \leqslant \bar{v}$	$v_a^l \geqslant \hat{v}$	$v_\epsilon^l \leqslant \hat{v}$	$(\hat{w}^l, \hat{v})$
				$v_\epsilon^l \geqslant \hat{v}$	(ϵ, v_ϵ^l)
			$v_a^l \leqslant \hat{v}$		(a, v_a^l)
		$v_a^u \leqslant \bar{v} \leqslant v_a^l$	$\hat{v} \leqslant \bar{v}$	$v_\epsilon^l \leqslant \hat{v}$	$(\hat{w}^l, \hat{v})$
				$\hat{v} \leqslant v_\epsilon^l \leqslant \bar{v}$	(ϵ, v_ϵ^l)
				$v_\epsilon^l \geqslant \bar{v}$	$(\epsilon, \bar{v})$
			$\hat{v} \geqslant \bar{v}$		$(a, \bar{v})$
		$\bar{v} \leqslant v_a^u \leqslant v_{max}$	$\hat{v} \leqslant \bar{v}$	$v_\epsilon^l \leqslant \hat{v}$	$(\hat{w}^l, \hat{v})$
				$\hat{v} \leqslant v_\epsilon^l \leqslant \bar{v}$	(ϵ, v_ϵ^l)
				$v_\epsilon^u \leqslant \bar{v} \leqslant v_\epsilon^l$	$(\epsilon, \bar{v})$
				$\bar{v} \leqslant v_\epsilon^u$	(ϵ, v_ϵ^u)
			$\bar{v} \leqslant \hat{v} \leqslant v_a^u$	$v_\epsilon^u \leqslant \hat{v}$	$(\hat{w}^u, \hat{v})$
				$v_\epsilon^u \geqslant \hat{v}$	(ϵ, v_ϵ^u)
			$\hat{v} \geqslant v_a^u$		(a, v_a^u)
		$v_a^u \geqslant v_{max}$	$\hat{v} \leqslant \bar{v}$	$v_\epsilon^l \leqslant \hat{v}$	$(\hat{w}^l, \hat{v})$
				$\hat{v} \leqslant v_\epsilon^l \leqslant \bar{v}$	(ϵ, v_ϵ^l)
				$v_\epsilon^u \leqslant \bar{v} \leqslant v_\epsilon^l$	$(\epsilon, \bar{v})$
				$\bar{v} \leqslant v_\epsilon^u$	(ϵ, v_ϵ^u)
			$\bar{v} \leqslant \hat{v} \leqslant v_{max}$	$v_\epsilon^u \leqslant \hat{v}$	$(\hat{w}^u, \hat{v})$
				$v_\epsilon^u \geqslant \hat{v}$	(ϵ, v_ϵ^u)
			$\hat{v} \geqslant v_{max}$		(w_{max}^u, v_{max})

Where $\hat{w}^l = a - (d - (l-a)\hat{v})/v_c, \hat{w}^u = a - (d - (u-a)\hat{v})/v_c$ and $\underline{w}^l = l - d/\underline{v}$.

Table A.12
Optimal solution when driver is paid from departure time.

Condition 1	Condition 2	Condition 3	Condition 4	Condition 5	Solution
$l \leqslant u \leqslant a$					(w, v_f) where $w \in \left[\max\left\{\epsilon, \left(l - \frac{d}{v_c}\right)\right\}, u - \frac{d}{v_c}\right]$
$l < a < u$	$v_{max} \leqslant \bar{v}$	$v_a^u \leqslant v_{max}$			(w, v_{max}) where $w \in [a, w_{max}^u]$
		$v_a^u \geqslant v_{max}$			(w_{max}^u, v_{max})
	$v_{max} \geqslant \bar{v}$	$v_a^u \leqslant \bar{v}$			$(w, \bar{v})$ where $w \in [a, \bar{w}^u]$
		$\bar{v} \leqslant v_a^u \leqslant v_{max}$	$\tilde{v} \leqslant v_a^u$	$v_\epsilon^u \leqslant \tilde{v}$	$(\tilde{w}^u, \tilde{v})$
				$v_\epsilon^u \geqslant \tilde{v}$	(ϵ, v_ϵ^u)
			$\tilde{v} \geqslant v_a^u$		(a, v_a^u)
		$v_a^u \geqslant v_{max}$	$\tilde{v} \leqslant v_{max}$	$v_\epsilon^u \leqslant \tilde{v}$	$(\tilde{w}^u, \tilde{v})$
				$v_\epsilon^u \geqslant \tilde{v}$	(ϵ, v_ϵ^u)
			$\tilde{v} \geqslant v_{max}$		(w_{max}^u, v_{max})
$a < l < u$	$v_{max} \leqslant \underline{v}$	$v_a^l \leqslant v_{max}$			(w, v_{max}) where $w \in [w_{max}^l, w_{max}^u]$
		$v_a^u \leqslant v_{max} \leqslant v_a^l$			(w, v_{max}) where $w \in [a, w_{max}^u]$
		$v_a^u \geqslant v_{max}$			(w_{max}^u, v_{max})
	$\underline{v} \leqslant v_{max} \leqslant \bar{v}$	$v_a^l \leqslant \underline{v}$			(w, v_{max}) where $w \in [w_{max}^l, w_{max}^u]$
		$\underline{v} \leqslant v_a^l \leqslant v_{max}$			(w, v_{max}) where $w \in [w_{max}^l, w_{max}^u]$
		$v_a^u \leqslant v_{max} \leqslant v_a^l$			(w, v_{max}) where $w \in [a, w_{max}^u]$
		$v_a^u \geqslant v_{max}$			(w_{max}^u, v_{max})
	$v_{max} \geqslant \bar{v}$	$v_a^l \leqslant \underline{v}$			$(w, \bar{v})$ where $w \in [\bar{w}^l, \bar{w}^u]$
		$\underline{v} \leqslant v_a^l \leqslant \bar{v}$			$(w, \bar{v})$ where $w \in [\bar{w}^l, \bar{w}^u]$
		$v_a^u \leqslant \bar{v} \leqslant v_a^l$			$(w, \bar{v})$ where $w \in [a, \bar{w}^u]$
		$\bar{v} \leqslant v_a^u \leqslant v_{max}$	$\tilde{v} \leqslant v_a^u$	$v_\epsilon^u \leqslant \tilde{v}$	$(\tilde{w}^u, \tilde{v})$
				$v_\epsilon^u \geqslant \tilde{v}$	(ϵ, v_ϵ^u)
			$\tilde{v} \geqslant v_a^u$		(a, v_a^u)
		$v_a^u \geqslant v_{max}$	$\tilde{v} \leqslant v_{max}$	$v_\epsilon^u \leqslant \tilde{v}$	$(\tilde{w}^u, \tilde{v})$
				$v_\epsilon^u \geqslant \tilde{v}$	(ϵ, v_ϵ^u)
			$\tilde{v} \geqslant v_{max}$		(w_{max}^u, v_{max})

Where $\tilde{w}^u = a - (d - (u - a)\tilde{v})/v_c$ and $\bar{w}^u = u - d/\bar{v}$.

$$
\begin{aligned}
TC_{s,e}(w_r, v_r; \epsilon_s) = {} & A\sum_{i=s}^{e-1} d_i + B\left(\sum_{i=s}^{r-1}\frac{d_i}{v_c} + (a - w_r)^+ + \frac{\left(d_r - (a - w_r)^+ v_c\right)^+}{v_r} + \sum_{i=r+1}^{e-1}\frac{d_i}{v_r}\right) \\
& + C\left[v_c^3\left(\sum_{i=s}^{r-1}\frac{d_i}{v_c} + \min\left\{\frac{d_r}{v_c}, (a - w_r)^+\right\}\right) + v_r^2\left(\left(d_r - (a - w_r)^+ v_c\right)^+ + \sum_{i=r+1}^{e-1} d_i\right)\right] \\
& + D\left(\max\left\{a + \frac{\left(d_r - (a - w_r)^+ v_c\right)^+}{v_r} + \sum_{i=r+1}^{e-1}\left(h_i + \frac{d_i}{v_r}\right), l_e\right\} + h_e - \epsilon_s\right).
\end{aligned}
\tag{B.1}
$$

The function *SINGLE_ARC_TDPRP* calculates the optimal departure time, i.e. w, and free flow speed, i.e. v, for a single-arc TDPRP with parameters $(a, v_c, v_{max}, d, \epsilon, l, u)$ using Theorem 5.1.

Appendix C. Proofs of lemmas and theorems

To simplify the notation in the proofs below, we let $A = f_c\lambda\gamma\alpha(\mu + f), B = f_c\lambda k N_e V$ and $C = f_c\lambda\beta\gamma, D = d_c$. Note that $A, B, C, D \geqslant 0$.

C.1. Proof of Lemma 5.1

Proof. First note that since $w \leqslant w_{max}^u$, we have $v_{max} \geqslant v_w^u$. For a fixed w, we need to minimize TC with respect to v_f in $\left[\max\left\{v_w^u, v_{min}\right\}, v_{max}\right]$.

When the driver is paid from the beginning of the time horizon, the total cost function TC for a fixed w as a function of the free-flow speed can be written as

$$
TC(w, v_f) = \begin{cases} Ad + \left(B + D + Cv_c^3\right)T_c(w) + \left(B + D + Cv_f^3\right)T_f(w, v_f) + D(w - \epsilon) & \text{if } \max\left\{v_w^u, v_{min}\right\} \leqslant v_f \leqslant \max\left\{v_w^l, v_{min}\right\} \\ Ad + \left(B + Cv_c^3\right)T_c(w) + \left(B + Cv_f^3\right)T_f(w, v_f) + D(l - \epsilon) & \text{if } v_f \geqslant \max\left\{v_w^l, v_{min}\right\}. \end{cases}
$$

For a fixed w, the function TC is continuous in v_f and is made of two pieces which are both convex in v_f. More precisely, the first piece is minimized at $v_f = \bar{v}$, while the second one at $v_f = \underline{v}$. Note that $\underline{v} < \bar{v}$.

In case (i) the first part is non-increasing and the second one is minimized at $\underline{v}$. If $\underline{v} > v_{max}$, the global minimum is achieved at v_{max}, otherwise it is achieved at $\max\{v_{min}, \underline{v}\}$. In case (ii) the first part is non-increasing and the second one is non-decreasing. If $v_w^l > v_{max}$, the global minimum is achieved at v_{max}, otherwise it is achieved at $\max\{v_{min}, v_w^l\}$. In case (iii) the first part is minimized at $\bar{v}$, while the second one is increasing. If $\bar{v} > v_{max}$, the global minimum is achieved at v_{max}, otherwise it is achieved at $\max\{v_{min}, \bar{v}\}$. Finally, in case (iv) both parts are non-decreasing so the global minimum is achieved at $\max\{v_{min}, v_w^u\}$.

When the driver is paid from his departure time, the total cost function has an extra $-D(w - \epsilon)$ term, which does not depend on v_f. Hence, the solution is the same. □

C.2. Proof of Theorem 5.1

Proof. In the following tables, we use circled numbers such as ① and ②, to refer to the pieces of the TC function. For each piece we use symbols such as →, ↗, ↘ and ⌣, to indicate whether the TC function is respectively constant, non-decreasing, non-increasing or convex, with respect to w.

Let $T(w) = \min_{v_f \in [v_{min}, v_{max}]} TC(w, v_f)$ such that $w + T(w, v_f) \leqslant u$. We consider three cases: (1) $l \leqslant u \leqslant a$, (2) $l < a < u$, and (3) $a \leqslant l < u$.

In case (1), we have:

$$TC(w) = \begin{cases} Ad + \left(B + Cv_c^3\right)\frac{d}{v_c} + D(l - \epsilon) & \text{if } \epsilon \leqslant w < \max\left\{\epsilon, l - \frac{d}{v_c}\right\} \\ Ad + \left(B + D + Cv_c^3\right)\frac{d}{v_c} + Dw & \text{if } \max\left\{\epsilon, l - \frac{d}{v_c}\right\} \leqslant w \leqslant u - \frac{d}{v_c}. \end{cases}$$

The first piece is constant in w and the second is increasing in w. So any departure time in $\left[\epsilon, \max\left\{\epsilon, l - \frac{d}{v_c}\right\}\right]$ is optimal. We summarize this information in Table C.13 where ① and ② are the time regions delimited by the breakpoints: $\max\left\{\epsilon, l - \frac{d}{v_c}\right\}$ and $u - \frac{d}{v_c}$.

In case (2), we distinguish two subcases: (2.1) $v_{max} < \bar{v}$, (2.2) $v_{max} \geqslant \bar{v}$.

In case (2.1):

$$TC(w) = \begin{cases} Ad + \left(B + Cv_c^3\right)\frac{d}{v_c} + D(l - \epsilon) & \text{if } \epsilon \leqslant w < \max\left\{\epsilon, l - \frac{d}{v_c}\right\} \\ Ad + \left(B + D + Cv_c^3\right)\frac{d}{v_c} + Dw & \text{if } \max\left\{\epsilon, l - \frac{d}{v_c}\right\} \leqslant w < \max\left\{\epsilon, a - \frac{d}{v_c}\right\} \\ Ad + \left(B + D + Cv_c^3\right)(a - w)^+ + (B + D + C(v_{max})^3)\frac{d - (a-w)^+ v_c}{v_{max}} + Dw & \text{if } \max\left\{\epsilon, a - \frac{d}{v_c}\right\} \leqslant w \leqslant w_{max}^u. \end{cases}$$

Table C.14 gives the solution depending on which piece contains the value a.

In some cases, there are two possible solutions. Then, the optimal solution can be obtained by calculating the cost associated with each one of them to find out which is the least (note that this needs to be done only if $\epsilon < a - \frac{d}{v_c}$, otherwise the solution with $w > \epsilon$ is the optimal one).

In case (2.2)

Table C.13
Case 1.

Case	①	②	Solution
1	→	↗	(w, v_f) with $w \in \left[\epsilon, \max\left\{\epsilon, l - \frac{d}{v_c}\right\}\right]$

Table C.14
Case 2.1.

Case	$a\in$	Condition 1	Condition 2	①	②	③	④	Solution
2.1.1.1	$\left[\max\left\{\epsilon, a - \frac{d}{v_c}\right\}, w_{max}^u\right)$	$v_a^u \leqslant v_{max}$	$\hat{v} \geqslant \check{v}$	→	↗	↘	↗	(a, v_{max}) or (ϵ, v_{max})
2.1.1.2	$\left[\max\left\{\epsilon, a - \frac{d}{v_c}\right\}, w_{max}^u\right)$	$v_a^u \leqslant v_{max}$	$\hat{v} \leqslant \check{v}$	→	↗	↗	↗	(ϵ, v_{max})
2.1.2.1	$[w_{max}^u, \infty)$	$v_a^u \geqslant v_{max}$	$\hat{v} \geqslant \check{v}$	→	↗	↘		(w_{max}^u, v_{max}) or (ϵ, v_{max})
2.1.2.2	$[w_{max}^u, \infty)$	$v_a^u \geqslant v_{max}$	$\hat{v} \leqslant \check{v}$	→	↗	↗		(ϵ, v_{max})

$$TC(w) = \begin{cases} Ad + \left(B + Cv_c^3\right)\frac{d}{v_c} + D(l-\epsilon) & \text{if } \epsilon \leqslant w < \max\left\{\epsilon, l - \frac{d}{v_c}\right\} \\ Ad + \left(B + D + Cv_c^3\right)\frac{d}{v_c} + Dw & \text{if } \max\left\{\epsilon, l - \frac{d}{v_c}\right\} \leqslant w < \max\left\{\epsilon, a - \frac{d}{v_c}\right\} \\ Ad + \left(B + D + Cv_c^3\right)(a-w)^+ + (B + D + C\bar{v}^3)\frac{d-(a-w)^+ v_c}{\bar{v}} + Dw & \text{if } \max\left\{\epsilon, a - \frac{d}{v_c}\right\} \leqslant w < \max\{\epsilon, \bar{w}^u\} \\ Ad + \left(B + D + Cv_c^3\right)(a-w)^+ + (B + D + C(v_w^u)^3)\frac{d-(a-w)^+ v_c}{v_w^u} + Dw & \text{if } \max\{\epsilon, \bar{w}^u\} \leqslant w \leqslant w_{max}^u. \end{cases}$$

where

$$\bar{w}^u = \begin{cases} a - \frac{d-(u-a)\bar{v}}{v_c} & \text{if } v_a^u \geqslant \bar{v} \\ u - \frac{d}{\bar{v}} & \text{otherwise.} \end{cases}$$

Table C.15 gives the solution in all possible subcases.
In case (3), we distinguish three subcases: (3.1) $v_{max} < \underline{v}$, (3.2) $\underline{v} \leqslant v_{max} < \bar{v}$, (3.3) $v_{max} \geqslant \bar{v}$.
In case (3.1)

$$TC(w) = \begin{cases} Ad + \left(B + Cv_c^3\right)\frac{d}{v_c} + D(l-\epsilon) & \text{if } \epsilon \leqslant w < \max\left\{\epsilon, \left(a - \frac{d}{v_c}\right)\right\} \\ Ad + \left(B + Cv_c^3\right)(a-w)^+ + (B + C(v_{max})^3)\frac{d-(a-w)^+ v_c}{v_{max}} + D(l-\epsilon) & \text{if } \max\left\{\epsilon, \left(a - \frac{d}{v_c}\right)\right\} \leqslant w < \max\{\epsilon, w_{max}^l\} \\ Ad + \left(B + D + Cv_c^3\right)(a-w)^+ + (B + D + C(v_{max})^3)\frac{d-(a-w)^+ v_c}{v_{max}} + Dw & \text{if } \max\{\epsilon, w_{max}^l\} \leqslant w \leqslant w_{max}^u. \end{cases}$$

Table C.16 gives the solution in all possible subcases.
In case (3.2)

$$TC(w) = \begin{cases} Ad + \left(B + Cv_c^3\right)\frac{d}{v_c} + D(l-\epsilon) & \text{if } \epsilon \leqslant w < \max\left\{\epsilon, \left(a - \frac{d}{v_c}\right)\right\} \\ Ad + \left(B + Cv_c^3\right)(a-w)^+ + (B + C\underline{v}^3)\frac{d-(a-w)^+ v_c}{\underline{v}} + D(l-\epsilon) & \text{if } \max\left\{\epsilon, \left(a - \frac{d}{v_c}\right)\right\} \leqslant w < \max\{\epsilon, \underline{w}^l\} \\ Ad + \left(B + Cv_c^3\right)(a-w)^+ + \left(B + C\left(v_w^l\right)^3\right)\frac{d-(a-w)^+ v_c}{v_w^l} + D(l-\epsilon) & \text{if } \max\{\epsilon, \underline{w}^l\} \leqslant w < \max\{\epsilon, w_{max}^l\} \\ Ad + \left(B + D + Cv_c^3\right)(a-w)^+ + (B + D + C(v_{max})^3)\frac{d-(a-w)^+ v_c}{v_{max}} + Dw & \text{if } \max\{\epsilon, (w_{max}^l)\} \leqslant w \leqslant w_{max}^u, \end{cases}$$

Table C.15
Case 2.2.

Case	$a \in$	Condition 1	Condition 2	Condition 3	①	②	③	④	⑤	Solution
2.2.1.1	$\left[\max\left\{\epsilon, a - \frac{d}{v_c}\right\}, \bar{w}^u\right)$	$v_a^u \leqslant \bar{v}$	$\hat{v} \geqslant \bar{v}$		→	↗	↘	↗	↗	$(a, \bar{v})$ or $(\epsilon, \bar{v})$
2.2.1.2	$\left[\max\left\{\epsilon, a - \frac{d}{v_c}\right\}, \bar{w}^u\right)$	$v_a^u \leqslant \bar{v}$	$\hat{v} \leqslant \bar{v}$		→	↗	↗	↗	↗	$(\epsilon, \bar{v})$
2.2.2.1.1	$[\bar{w}^u, w_{max}^u)$	$\bar{v} \leqslant v_a^u \leqslant v_{max}$	$\hat{v} \leqslant \bar{v}$	$v_\epsilon^u \leqslant \bar{v}$	→	↗	↗	↗	↗	$(\epsilon, \bar{v})$
2.2.2.1.2	$[\bar{w}^u, w_{max}^u)$	$\bar{v} \leqslant v_a^u \leqslant v_{max}$	$\hat{v} \leqslant \bar{v}$	$v_\epsilon^u \geqslant \bar{v}$	↗	↗				(ϵ, v_ϵ^u)
2.2.2.2.1	$[\bar{w}^u, w_{max}^u)$	$\bar{v} \leqslant v_a^u \leqslant v_{max}$	$\bar{v} \leqslant \hat{v} \leqslant v_a^u$	$v_\epsilon^u \leqslant \hat{v}$	→	↗	↘	⌣	↗	$(\hat{w}^u, \hat{v})$ or $(\epsilon, \bar{v})$
2.2.2.2.2	$[\bar{w}^u, w_{max}^u)$	$\bar{v} \leqslant v_a^u \leqslant v_{max}$	$\bar{v} \leqslant \hat{v} \leqslant v_a^u$	$v_\epsilon^u \geqslant \hat{v}$	↗	↗				(ϵ, v_ϵ^u)
2.2.2.3	$[\bar{w}^u, w_{max}^u)$	$\bar{v} \leqslant v_a^u \leqslant v_{max}$	$\hat{v} \geqslant v_a^u$		→	↗	↘	↘	↗	(a, v_u^a) or $(\epsilon, \bar{v})$
2.2.3.1.1	$[w_{max}^u, \infty)$	$v_a^u \geqslant v_{max}$	$\hat{v} \leqslant \bar{v}$	$v_\epsilon^u \leqslant \bar{v}$	→	↗	↗	↗		$(\epsilon, \bar{v})$
2.2.3.1.2	$[w_{max}^u, \infty)$	$v_a^u \geqslant v_{max}$	$\hat{v} \leqslant \bar{v}$	$v_\epsilon^u \geqslant \bar{v}$	↗	↗				(ϵ, v_ϵ^u)
2.2.3.2.1	$[w_{max}^u, \infty)$	$v_a^u \geqslant v_{max}$	$\bar{v} \leqslant \hat{v} \leqslant v_{max}$	$v_\epsilon^u \leqslant \hat{v}$	→	↗	↘	⌣		$(\hat{w}^u, \hat{v})$ or $(\epsilon, \bar{v})$
2.2.3.2.2	$[w_{max}^u, \infty)$	$v_a^u \geqslant v_{max}$	$\bar{v} \leqslant \hat{v} \leqslant v_{max}$	$v_\epsilon^u \geqslant \hat{v}$	↗					(ϵ, v_ϵ^u)
2.2.3.3	$[w_{max}^u, \infty)$	$v_a^u \geqslant v_{max}$	$\hat{v} \geqslant v_{max}$		→	↗	↘	↘		(w_{max}^u, v_{max}) or $(\epsilon, \bar{v})$

Where $\hat{w}^u = a - (d - (u-a)\hat{v})/v_c$.

Table C.16
Case 3.1.

Case	$a \in$	Condition 1	Condition 2	①	②	③	④	Solution
3.1.1	$\left[\max\left\{\epsilon, \left(a - \frac{d}{v_c}\right)\right\}, \max\{\epsilon, w_{max}^l\}\right)$	$v_a^l \leqslant v_{max}$		→	↘	→	↗	(w, v_{max}) where $w \in [a, w_{max}^l]$
3.1.2.1	$[w_{max}^l, w_{max}^u]$	$v_a^u \leqslant v_{max} \leqslant v_a^l$	$\check{v} \leqslant \hat{v}$	→	↘	↘	↗	(a, v_{max})
3.1.2.1	$[w_{max}^l, w_{max}^u]$	$v_a^u \leqslant v_{max} \leqslant v_a^l$	$\check{v} \geqslant \hat{v}$	→	↘	↗	↗	$(\max\{\epsilon, w_{max}^l\}, v_{max})$
3.1.3.1	$[w_{max}^u, \infty)$	$v_a^u \geqslant v_{max}$	$\check{v} \leqslant \hat{v}$	→	↘	↘		(w_{max}^u, v_{max})
3.1.3.2	$[w_{max}^u, \infty)$	$v_a^u \geqslant v_{max}$	$\check{v} \geqslant \hat{v}$	→	↘	↗		$(\max\{\epsilon, w_{max}^l\}, v_{max})$

where

$$\underline{w}^l = \begin{cases} a - \frac{d-(l-a)\underline{v}}{v_c} & \text{if } v_a^l \geqslant \underline{v} \\ l - \frac{d}{\underline{v}} & \text{otherwise.} \end{cases}$$

Table C.17 gives the solution in all possible subcases.

In case (3.3):

$$TC(w) = \begin{cases} Ad + \left(B + Cv_c^3\right)\frac{d}{v_c} + D(l-\epsilon) & \text{if } \epsilon \leqslant w < \max\left\{\epsilon, \left(a - \frac{d}{v_c}\right)\right\} \\ Ad + \left(B + Cv_c^3\right)(a-w)^+ + (B + C\underline{v}^3)\frac{d-(a-w)^+ v_c}{\underline{v}} + D(l-\epsilon) & \text{if } \max\left\{\epsilon, \left(a - \frac{d}{v_c}\right)\right\} \leqslant w < \max\{\epsilon, \underline{w}^l\} \\ Ad + \left(B + Cv_c^3\right)(a-w)^+ + (B + C(v_w^l)^3)\frac{d-(a-w)^+ v_c}{v_w^l} + D(l-\epsilon) & \text{if } \max\{\epsilon, \underline{w}^l\} \leqslant w < \max\{\epsilon, \bar{w}^l\} \\ Ad + \left(B + D + Cv_c^3\right)(a-w)^+ + (B + D + C\bar{v}^3)\frac{d-(a-w)^+ v_c}{\bar{v}} + Dw & \text{if } \max\{\epsilon, \bar{w}^l\} \leqslant w < \max\{\epsilon, \bar{w}^u\} \\ Ad + \left(B + D + Cv_c^3\right)(a-w)^+ + (B + D + C(v_w^u)^3)\frac{d-(a-w)^+ v_c}{v_w^u} + Dw & \text{if } \max\{\epsilon, \bar{w}^u\} \leqslant w \leqslant w_{max}^u \end{cases}$$

where

$$\bar{w}^l = \begin{cases} a - \frac{d-(l-a)\bar{v}}{v_c} & \text{if } v_a^l \geqslant \bar{v} \\ l - \frac{d}{\bar{v}} & \text{otherwise.} \end{cases}$$

Table C.18 gives the solution for all subcases. □

C.3. Proof of Theorem 5.2

Proof. Let $T(w) = \min_{v_f \in [v_{min}, v_{max}]} TC(w, v_f)$ such that $w + T(w, v_f) \leqslant u$. We consider three cases: (1) $l \leqslant u \leqslant a$, (2) $l < a < u$, and (3) $a \leqslant l < u$.

In case (1), we have

$$TC(w) = \begin{cases} Ad + \left(B + Cv_c^3\right)\frac{d}{v_c} + D(l-w) & \text{if } \epsilon \leqslant w < \max\left\{\epsilon, l - \frac{d}{v_c}\right\} \\ Ad + \left(B + D + Cv_c^3\right)\frac{d}{v_c} & \text{if } \max\left\{\epsilon, l - \frac{d}{v_c}\right\} \leqslant w \leqslant u - \frac{d}{v_c}. \end{cases}$$

The first piece is decreasing in w and the second is constant in w. So any departure time in $\left[\max\left\{\epsilon, l - \frac{d}{v_c}\right\}, u\right]$ is optimal. We summarize this information in Table C.19.

In case 2 we distinguish two subcases: (2.1) $v_{max} < \bar{v}$, (2.2) $v_{max} \geqslant \bar{v}$.

In case (2.1)

Table C.17
Case 3.2.

Case	$a \in$	Condition 1	Condition 2	Condition 3	①	②	③	④	⑤	Solution
3.2.1	$\left[\max\left\{\epsilon, \left(a - \frac{d}{v_c}\right)\right\}, \underline{w}^l\right)$	$v_a^l \leqslant \underline{v}$			$\rightarrow$	$\searrow$	$\rightarrow$	$\nearrow$	$\nearrow$	$(w, \underline{v})$ where $w \in [a, \underline{w}^l]$
3.2.2.1.1	$[\underline{w}^l, w_{max}^l)$	$\underline{v} \leqslant v_a^l \leqslant v_{max}$	$v_a^l \geqslant \hat{v}$	$v_\epsilon^l \leqslant \hat{v}$	$\rightarrow$	$\searrow$	$\smile$	$\nearrow$	$\nearrow$	$(\hat{w}^l, \hat{v})$
3.2.2.1.2	$[\underline{w}^l, w_{max}^l)$	$\underline{v} \leqslant v_a^l \leqslant v_{max}$	$v_a^l \geqslant \hat{v}$	$v_\epsilon^l \geqslant \hat{v}$	$\nearrow$	$\nearrow$	$\nearrow$			(ϵ, v_ϵ^l)
3.2.2.2	$[\underline{w}^l, w_{max}^l)$	$\underline{v} \leqslant v_a^l \leqslant v_{max}$	$v_a^l \leqslant \hat{v}$		$\rightarrow$	$\searrow$	$\searrow$	$\nearrow$	$\nearrow$	(a, v_a^l)
3.2.3.1.1	$[w_{max}^l, w_{max}^u)$	$v_a^u \leqslant v_{max} \leqslant v_a^l$	$\hat{v} \leqslant v_{max}$	$v_\epsilon^l \leqslant \hat{v}$	$\rightarrow$	$\searrow$	$\smile$	$\nearrow$	$\nearrow$	$(\hat{w}^l, \hat{v})$
3.2.3.1.2	$[w_{max}^l, w_{max}^u)$	$v_a^u \leqslant v_{max} \leqslant v_a^l$	$\hat{v} \leqslant v_{max}$	$\hat{v} \leqslant v_\epsilon^l \leqslant v_{max}$	$\nearrow$	$\nearrow$	$\nearrow$			(ϵ, v_ϵ^l)
3.2.3.1.3	$[w_{max}^l, w_{max}^u)$	$v_a^u \leqslant v_{max} \leqslant v_a^l$	$\hat{v} \leqslant v_{max}$	$v_\epsilon^l \geqslant v_{max}$	$\nearrow$	$\nearrow$				(ϵ, v_{max})
3.2.3.2.1	$[w_{max}^l, w_{max}^u)$	$v_a^u \leqslant v_{max} \leqslant v_a^l$	$v_{max} \leqslant \hat{v} \leqslant \check{v}$	$v_\epsilon^l \leqslant v_{max}$	$\rightarrow$	$\searrow$	$\searrow$	$\nearrow$	$\nearrow$	(w_{max}^l, v_{max})
3.2.3.2.2	$[w_{max}^l, w_{max}^u)$	$v_a^u \leqslant v_{max} \leqslant v_a^l$	$v_{max} \leqslant \hat{v} \leqslant \check{v}$	$v_\epsilon^l \geqslant v_{max}$	$\nearrow$	$\nearrow$				(ϵ, v_{max})
3.2.3.3	$[w_{max}^l, w_{max}^u)$	$v_a^u \leqslant v_{max} \leqslant v_a^l$	$\hat{v} \geqslant \check{v}$		$\rightarrow$	$\searrow$	$\searrow$	$\searrow$	$\nearrow$	(a, v_{max})
3.2.4.1.1	$[w_{max}^u, \infty)$	$v_a^u \geqslant v_{max}$	$\hat{v} \leqslant v_{max}$	$v_\epsilon^l \leqslant \hat{v}$	$\rightarrow$	$\searrow$	$\smile$	$\nearrow$		$(\hat{w}^l, \hat{v})$
3.2.4.1.2	$[w_{max}^u, \infty)$	$v_a^u \geqslant v_{max}$	$\hat{v} \leqslant v_{max}$	$\hat{v} \leqslant v_\epsilon^l \leqslant v_{max}$	$\nearrow$	$\nearrow$				(ϵ, v_ϵ^l)
3.2.4.1.3	$[w_{max}^u, \infty)$	$v_a^u \geqslant v_{max}$	$\hat{v} \leqslant v_{max}$	$v_\epsilon^l \geqslant v_{max}$	$\nearrow$					(ϵ, v_{max})
3.2.4.2.1	$[w_{max}^u, \infty)$	$v_a^u \geqslant v_{max}$	$v_{max} \leqslant \hat{v} \leqslant \check{v}$	$v_\epsilon^l \leqslant v_{max}$	$\rightarrow$	$\searrow$	$\searrow$	$\nearrow$		(w_{max}^l, v_{max})
3.2.4.2.2	$[w_{max}^u, \infty)$	$v_a^u \geqslant v_{max}$	$v_{max} \leqslant \hat{v} \leqslant \check{v}$	$v_\epsilon^l \geqslant v_{max}$	$\nearrow$					(ϵ, v_{max})
3.2.4.3	$[w_{max}^u, \infty)$	$v_a^u \geqslant v_{max}$	$\hat{v} \geqslant \check{v}$		$\rightarrow$	$\searrow$	$\searrow$	$\searrow$		(w_{max}^u, v_{max})

Where $\hat{w}^l = a - (d - (l-a)\hat{v})/v_c$.

Table C.18
Case 3.3.

Case	$a\in$	Condition 1	Condition 2	Condition 3	①	②	③	④	⑤	⑥	Solution
3.3.1	$\left[\max\left\{\epsilon,\left(a-\frac{d}{v_c}\right)\right\},\underline{v}^l\right)$	$v_a^l \leqslant \underline{v}$			$\rightarrow$	$\searrow$	$\rightarrow$	$\nearrow$	$\nearrow$	$\nearrow$	$(w,\underline{v})$ where $w\in[a,\underline{w}^l]$
3.3.2.1.1	$[\underline{w}^l,\bar{w}^l)$	$\underline{v}\leqslant v_a^l\leqslant\bar{v}$	$v_a^l \geqslant \hat{v}$	$v_\epsilon^l\leqslant\hat{v}$	$\rightarrow$	$\searrow$	$\smile$	$\nearrow$	$\nearrow$	$\nearrow$	$(\hat{w}^l,\hat{v})$
3.3.2.1.2	$[\underline{w}^l,\bar{w}^l)$	$\underline{v}\leqslant v_a^l\leqslant\bar{v}$	$v_a^l \geqslant \hat{v}$	$v_\epsilon^l\geqslant\hat{v}$	$\nearrow$	$\nearrow$	$\nearrow$	$\nearrow$			(ϵ,v_ϵ^l)
3.3.2.2	$[\underline{w}^l,\bar{w}^l)$	$\underline{v}\leqslant v_a^l\leqslant\bar{v}$	$v_a^l \leqslant \hat{v}$		$\rightarrow$	$\searrow$	$\searrow$	$\nearrow$	$\nearrow$	$\nearrow$	(a,v_a^l)
3.3.3.1.1	$[\bar{w}^l,\bar{w}^u)$	$v_a^u\leqslant\bar{v}\leqslant v_a^l$	$\hat{v}\leqslant\bar{v}$	$v_\epsilon^l\leqslant\hat{v}$	$\rightarrow$	$\searrow$	$\smile$	$\nearrow$	$\nearrow$	$\nearrow$	$(\hat{w}^l,\hat{v})$
3.3.3.1.2	$[\bar{w}^l,\bar{w}^u)$	$v_a^u\leqslant\bar{v}\leqslant v_a^l$	$\hat{v}\leqslant\bar{v}$	$\hat{v}\leqslant v_\epsilon^l\leqslant\bar{v}$	$\nearrow$	$\nearrow$	$\nearrow$	$\nearrow$			(ϵ,v_ϵ^l)
3.3.3.1.3	$[\bar{w}^l,\bar{w}^u)$	$v_a^u\leqslant\bar{v}\leqslant v_a^l$	$\hat{v}\leqslant\bar{v}$	$v_\epsilon^l\geqslant\bar{v}$	$\nearrow$	$\nearrow$	$\nearrow$				$(\epsilon,\bar{v})$
3.3.3.2	$[\bar{w}^l,\bar{w}^u)$	$v_a^u\leqslant\bar{v}\leqslant v_a^l$	$\hat{v}\geqslant\bar{v}$		$\rightarrow$	$\searrow$	$\searrow$	$\searrow$	$\nearrow$	$\nearrow$	$(a,\bar{v})$
3.3.4.1.1	$[\bar{w}^u,w_{max}^u)$	$\bar{v}\leqslant v_a^u\leqslant v_{max}$	$\hat{v}\leqslant\bar{v}$	$v_\epsilon^l\leqslant\hat{v}$	$\rightarrow$	$\searrow$	$\smile$	$\nearrow$	$\nearrow$	$\nearrow$	$(\hat{w}^l,\hat{v})$
3.3.4.1.2	$[\bar{w}^u,w_{max}^u)$	$\bar{v}\leqslant v_a^u\leqslant v_{max}$	$\hat{v}\leqslant\bar{v}$	$\hat{v}\leqslant v_\epsilon^l\leqslant\bar{v}$	$\nearrow$	$\nearrow$	$\nearrow$	$\nearrow$			(ϵ,v_ϵ^l)
3.3.4.1.3	$[\bar{w}^u,w_{max}^u)$	$\bar{v}\leqslant v_a^u\leqslant v_{max}$	$\hat{v}\leqslant\bar{v}$	$v_\epsilon^u\leqslant\bar{v}\leqslant v_\epsilon^l$	$\nearrow$	$\nearrow$	$\nearrow$				$(\epsilon,\bar{v})$
3.3.4.1.4	$[\bar{w}^u,w_{max}^u)$	$\bar{v}\leqslant v_a^u\leqslant v_{max}$	$\hat{v}\leqslant\bar{v}$	$\bar{v}\leqslant v_\epsilon^u$	$\nearrow$	$\nearrow$					(ϵ,v_ϵ^u)
3.3.4.2.1	$[\bar{w}^u,w_{max}^u)$	$\bar{v}\leqslant v_a^u\leqslant v_{max}$	$\bar{v}\leqslant\hat{v}\leqslant v_a^u$	$v_\epsilon^u\leqslant\hat{v}$	$\rightarrow$	$\searrow$	$\searrow$	$\searrow$	$\smile$	$\nearrow$	$(\hat{w}^u,\hat{v})$
3.3.4.2.2	$[\bar{w}^u,w_{max}^u)$	$\bar{v}\leqslant v_a^u\leqslant v_{max}$	$\bar{v}\leqslant\hat{v}\leqslant v_a^u$	$v_\epsilon^u\geqslant\hat{v}$	$\nearrow$	$\nearrow$					(ϵ,v_ϵ^u)
3.3.4.3	$[\bar{w}^u,w_{max}^u)$	$\bar{v}\leqslant v_a^u\leqslant v_{max}$	$\hat{v}\geqslant v_a^u$		$\rightarrow$	$\searrow$	$\searrow$	$\searrow$	$\searrow$	$\nearrow$	(a,v_a^u)
3.3.5.1.1	$[w_{max}^u,\infty)$	$v_a^u\geqslant v_{max}$	$\hat{v}\leqslant\bar{v}$	$v_\epsilon^l\leqslant\hat{v}$	$\rightarrow$	$\searrow$	$\smile$	$\nearrow$	$\nearrow$		$(\hat{w}^l,\hat{v})$
3.3.5.1.2	$[w_{max}^u,\infty)$	$v_a^u\geqslant v_{max}$	$\hat{v}\leqslant\bar{v}$	$\hat{v}\leqslant v_\epsilon^l\leqslant\bar{v}$	$\nearrow$	$\nearrow$	$\nearrow$				(ϵ,v_ϵ^l)
3.3.5.1.3	$[w_{max}^u,\infty)$	$v_a^u\geqslant v_{max}$	$\hat{v}\leqslant\bar{v}$	$v_\epsilon^u\leqslant\bar{v}\leqslant v_\epsilon^l$	$\nearrow$	$\nearrow$					$(\epsilon,\bar{v})$
3.3.5.1.4	$[w_{max}^u,\infty)$	$v_a^u\geqslant v_{max}$	$\hat{v}\leqslant\bar{v}$	$\bar{v}\leqslant v_\epsilon^u$	$\nearrow$						(ϵ,v_ϵ^u)
3.3.5.2.1	$[w_{max}^u,\infty)$	$v_a^u\geqslant v_{max}$	$\bar{v}\leqslant\hat{v}\leqslant v_{max}$	$v_\epsilon^u\leqslant\hat{v}$	$\rightarrow$	$\searrow$	$\searrow$	$\searrow$	$\smile$		$(\hat{w}^u,\hat{v})$
3.3.5.2.2	$[w_{max}^u,\infty)$	$v_a^u\geqslant v_{max}$	$\bar{v}\leqslant\hat{v}\leqslant v_{max}$	$v_\epsilon^u\geqslant\hat{v}$	$\nearrow$						(ϵ,v_ϵ^u)
3.3.5.3	$[w_{max}^u,\infty)$	$v_a^u\geqslant v_{max}$	$\hat{v}\geqslant v_{max}$		$\rightarrow$	$\searrow$	$\searrow$	$\searrow$	$\searrow$		(w_{max}^u,v_{max})

Where $\hat{w}^u=a-(d-(u-a)\hat{v})/v_c$ and $\hat{w}^l=a-(d-(l-a)\hat{v})/v_c$.

Table C.19
Case 1.

Case	①	②	Solution
1	$\searrow$	$\rightarrow$	(w,v_f) with $w\in\left[\max\left\{\epsilon,l-\frac{d}{v_c}\right\},u-\frac{d}{v_c}\right]$

Table C.20
Case 2.1.

Case	$a\in$	Condition 1	①	②	③	④	Solution
2.1.1	$\left[\max\left\{\epsilon,\left(a-\frac{d}{v_c}\right)\right\},w_{max}^u\right)$	$v_a^u\leqslant v_{max}$	$\searrow$	$\rightarrow$	$\searrow$	$\rightarrow$	(w,v_{max}) where $w\in[a,w_{max}^u]$
2.1.2	$[w_{max}^u,\infty)$	$v_a^u\geqslant v_{max}$	$\searrow$	$\rightarrow$	$\searrow$		(w_{max}^u,v_{max})

$$TC(w)=\begin{cases} Ad+\left(B+Cv_c^3\right)\frac{d}{v_c}+D(l-w) & \text{if } \epsilon\leqslant w<\max\left\{\epsilon,l-\frac{d}{v_c}\right\}\\ Ad+\left(B+D+Cv_c^3\right)\frac{d}{v_c} & \text{if } \max\left\{\epsilon,l-\frac{d}{v_c}\right\}\leqslant w<\max\left\{\epsilon,\left(a-\frac{d}{v_c}\right)\right\}\\ Ad+\left(B+D+Cv_c^3\right)(a-w)^+ +\left(B+D+C(v_{max})^3\right)\frac{d-(a-w)^+v_c}{v_{max}} & \text{if } \max\left\{\epsilon,\left(a-\frac{d}{v_c}\right)\right\}\leqslant w\leqslant w_{max}^u. \end{cases}$$

Table C.20 gives the solution in all possible subcases.
In case (2.2)

$$TC(w)=\begin{cases} Ad+\left(B+Cv_c^3\right)\frac{d}{v_c}+D(l-w) & \text{if } \epsilon\leqslant w<\max\left\{\epsilon,l-\frac{d}{v_c}\right\}\\ Ad+\left(B+D+Cv_c^3\right)\frac{d}{v_c} & \text{if } \max\left\{\epsilon,l-\frac{d}{v_c}\right\}\leqslant w<\max\left\{\epsilon,\left(a-\frac{d}{v_c}\right)\right\}\\ Ad+\left(B+D+Cv_c^3\right)(a-w)^+ +\left(B+D+C\bar{v}^3\right)\frac{d-(a-w)^+v_c}{\bar{v}} & \text{if } \max\left\{\epsilon,\left(a-\frac{d}{v_c}\right)\right\}\leqslant w<\max\left\{\epsilon,\bar{w}^u\right\}\\ Ad+\left(B+D+Cv_c^3\right)(a-w)^+ +\left(B+D+C\left(v_w^u\right)^3\right)\frac{d-(a-w)^+v_c}{v_w^u} & \text{if } \max\{\epsilon,\bar{w}^u\}\leqslant w\leqslant w_{max}^u. \end{cases}$$

Table C.21 gives the solution in all possible subcases.

Table C.21
Case 2.2.

Case	$a\in$	Condition 1	Condition 2	Condition 3	①	②	③	④	⑤	Solution
2.2.1	$\left[\max\left\{\epsilon, \left(a-\frac{d}{v_c}\right)\right\}, \bar{w}^u\right)$	$v_a^u \leqslant \bar{v}$			$\searrow$	$\rightarrow$	$\searrow$	$\rightarrow$	$\nearrow$	$(w, \bar{v})$ where $w \in [a, \bar{w}^u)$
2.2.2.1.1	$[\bar{w}^u, w^u_{max})$	$\bar{v} \leqslant v_a^u \leqslant v_{max}$	$\tilde{v} \leqslant v_a^u$	$v_\epsilon^u \leqslant \tilde{v}$	$\searrow$	$\rightarrow$	$\searrow$	$\smile$	$\nearrow$	$(\tilde{w}^u, \tilde{v})$
2.2.2.1.2	$[\bar{w}^u, w^u_{max})$	$\bar{v} \leqslant v_a^u \leqslant v_{max}$	$\tilde{v} \leqslant v_a^u$	$v_\epsilon^u \geqslant \tilde{v}$	$\nearrow$	$\nearrow$				(ϵ, v_ϵ^u)
2.2.2.2	$[\bar{w}^u, w^u_{max})$	$\bar{v} \leqslant v_a^u \leqslant v_{max}$	$\tilde{v} \geqslant v_a^u$		$\searrow$	$\rightarrow$	$\searrow$	$\searrow$	$\nearrow$	(a, v_a^u)
2.2.3.1.1	$[w^u_{max}, \infty)$	$v_a^u \geqslant v_{max}$	$\tilde{v} \leqslant v_{max}$	$v_\epsilon^u \leqslant \tilde{v}$	$\searrow$	$\rightarrow$	$\searrow$	$\smile$		$(\tilde{w}^u, \tilde{v})$
2.2.3.1.2	$[w^u_{max}, \infty)$	$v_a^u \geqslant v_{max}$	$\tilde{v} \leqslant v_{max}$	$v_\epsilon^u \geqslant \tilde{v}$	$\nearrow$					(ϵ, v_ϵ^u)
2.2.3.2	$[w^u_{max}, \infty)$	$v_a^u \geqslant v_{max}$	$\tilde{v} \geqslant v_{max}$		$\searrow$	$\rightarrow$	$\searrow$	$\searrow$		(w^u_{max}, v_{max})

Where $\tilde{w}^u = a - (d - (u-a)\tilde{v})/v_c$.

In case 3 we distinguish three subcases: (3.1) $v_{max} < \underline{v}$, (3.2) $\underline{v} \leqslant v_{max} < \bar{v}$, (3.3) $v_{max} \geqslant \bar{v}$.
In case (3.1)

$$TC(w) = \begin{cases} Ad + \left(B + Cv_c^3\right)\frac{d}{v_c} + D(l-w) & \text{if } \epsilon \leqslant w < \max\left\{\epsilon, \left(a - \frac{d}{v_c}\right)\right\} \\ Ad + \left(B + Cv_c^3\right)(a-w)^+ + (B + C(v_{max})^3)\frac{d-(a-w)^+ v_c}{v_{max}} + D(l-w) & \text{if } \max\left\{\epsilon, \left(a - \frac{d}{v_c}\right)\right\} \leqslant w < \max\{\epsilon, w^l_{max}\} \\ Ad + \left(B + D + Cv_c^3\right)(a-w)^+ + (B + D + C(v_{max})^3)\frac{d-(a-w)^+ v_c}{v_{max}} & \text{if } \max\{\epsilon, w^l_{max}\} \leqslant w \leqslant w^u_{max}. \end{cases}$$

Table C.22 gives the solution in all possible subcases.
In case (3.2)

$$TC(w) = \begin{cases} Ad + \left(B + Cv_c^3\right)\frac{d}{v_c} + D(l-w) & \text{if } \epsilon \leqslant w < \max\left\{\epsilon, \left(a - \frac{d}{v_c}\right)\right\} \\ Ad + \left(B + Cv_c^3\right)(a-w)^+ + (B + C\underline{v}^3)\frac{d-(a-w)^+ v_c}{\underline{v}} + D(l-w) & \text{if } \max\left\{\epsilon, \left(a - \frac{d}{v_c}\right)\right\} \leqslant w < \max\{\epsilon, \underline{w}^l\} \\ Ad + \left(B + Cv_c^3\right)(a-w)^+ + (B + C(v_w^l)^3)\frac{d-(a-w)^+ v_c}{v_w^l} + D(l-w) & \text{if } \max\{\epsilon, \underline{w}^l\} \leqslant w < \max\{\epsilon, w^l_{max}\} \\ Ad + (B + D + Cv_c^3)(a-w)^+ + (B + D + C(v_{max})^3)\frac{d-(a-w)^+ v_c}{v_{max}} & \text{if } \max\{\epsilon, w^l_{max}\} \leqslant w \leqslant w^u_{max}. \end{cases}$$

Table C.23 gives the solution in all possible subcases.
In case (3.3)

$$TC(w) = \begin{cases} Ad + \left(B + Cv_c^3\right)\frac{d}{v_c} + Dl & \text{if } \epsilon \leqslant w < \max\left\{\epsilon, \left(a - \frac{d}{v_c}\right)\right\} \\ Ad + \left(B + Cv_c^3\right)(a-w)^+ + (B + C\underline{v}^3)\frac{d-(a-w)^+ v_c}{\underline{v}} + D(l-w) & \text{if } \max\left\{\epsilon, \left(a - \frac{d}{v_c}\right)\right\} \leqslant w < (\underline{w}^l)^+ \\ Ad + \left(B + Cv_c^3\right)(a-w)^+ + (B + C(v_w^l)^3)\frac{d-(a-w)^+ v_c}{v_w^l} + D(l-w) & \text{if } (\underline{w}^l)^+ \leqslant w < (\bar{w}^l)^+ \\ Ad + (B + D + Cv_c^3)(a-w)^+ + (B + D + C\bar{v}^3)\frac{d-(a-w)^+ v_c}{\bar{v}} & \text{if } (\bar{w}^l)^+ \leqslant w < (\bar{w}^u)^+ \\ Ad + (B + D + Cv_c^3)(a-w)^+ + (B + D + C(v_w^u)^3)\frac{d-(a-w)^+ v_c}{v_w^u} & \text{if } (\bar{w}^u)^+ \leqslant w \leqslant w^u_{max}. \end{cases}$$

Table C.22
Case 3.1.

Case	$a\in$	Condition 1	①	②	③	④	Solution
3.1.1	$\left[\max\left\{\epsilon, \left(a-\frac{d}{v_c}\right)\right\}, w^l_{max}\right)$	$v_a^l \leqslant v_{max}$	$\searrow$	$\searrow$	$\searrow$	$\rightarrow$	(w, v_{max}) where $w \in [w^l_{max}, w^u_{max}]$
3.1.2	$[w^l_{max}, w^u_{max})$	$v_a^u \leqslant v_{max} \leqslant v_a^l$	$\searrow$	$\searrow$	$\searrow$	$\rightarrow$	(w, v_{max}) where $w \in [a, w^u_{max}]$
3.1.3	$[w^l_{max}, w^u_{max})$	$v_a^u \geqslant v_{max}$	$\searrow$	$\searrow$	$\searrow$		(w^u_{max}, v_{max}).

Table C.23
Case 3.2.

Case	$a\in$	Condition 1	①	②	③	④	⑤	Solution
3.2.1	$\left[\max\left\{\epsilon, \left(a-\frac{d}{v_c}\right)\right\}, \underline{w}^l\right)$	$v_a^l \leqslant \underline{v}$	$\searrow$	$\searrow$	$\searrow$	$\searrow$	$\rightarrow$	(w, v_{max}) where $w \in [w^l_{max}, w^u_{max}]$
3.2.2	$[\underline{w}^l, w^l_{max})$	$\underline{v} \leqslant v_a^l \leqslant v_{max}$	$\searrow$	$\searrow$	$\searrow$	$\searrow$	$\rightarrow$	(w, v_{max}) where $w \in [w^l_{max}, w^u_{max}]$
3.2.3	$[w^l_{max}, w^u_{max})$	$v_a^u \leqslant v_{max} \leqslant v_a^l$	$\searrow$	$\searrow$	$\searrow$	$\searrow$	$\rightarrow$	(w, v_{max}) where $w \in [a, w^u_{max}]$
3.2.4	$[w^u_{max}, \infty)$	$v_a^u \geqslant v_{max}$	$\searrow$	$\searrow$	$\searrow$	$\searrow$		(w^u_{max}, v_{max})

Table C.24
Case 3.3.

Case	$a\in$	Condition 1	Condition 2	Condition 3	①	②	③	④	⑤	⑥	Solution
3.3.1	$\left[\max\left\{\epsilon, \left(a - \frac{d}{v_c}\right)\right\}, \underline{w}^l\right)$	$v_a^l \leqslant \underline{v}$			$\searrow$	$\searrow$	$\searrow$	$\searrow$	$\rightarrow$	$\nearrow$	$(w, \bar{v})$ where $w \in [\bar{w}^l, \bar{w}^u]$
3.3.2	$[\underline{w}^l, \bar{w}^l)$	$\underline{v} \leqslant v_a^l \leqslant \bar{v}$			$\searrow$	$\searrow$	$\searrow$	$\searrow$	$\rightarrow$	$\nearrow$	$(w, \bar{v})$ where $w \in [\bar{w}^l, \bar{w}^u]$
3.3.3	$[\bar{w}^l, \bar{w}^u)$	$v_a^u \leqslant \bar{v} \leqslant v_a^l$			$\searrow$	$\searrow$	$\searrow$	$\searrow$	$\rightarrow$	$\nearrow$	$(w, \bar{v})$ where $w \in [a, \bar{w}^u]$
3.3.4.1.1	$[\bar{w}^u, w_{max}^u)$	$\bar{v} \leqslant v_a^u \leqslant v_{max}$	$\tilde{v} \leqslant v_a^u$	$v_\epsilon^u \leqslant \tilde{v}$	$\searrow$	$\searrow$	$\searrow$	$\searrow$	$\smile$	$\nearrow$	$(\tilde{w}^u, \tilde{v})$
3.3.4.1.2	$[\bar{w}^u, w_{max}^u)$	$\bar{v} \leqslant v_a^u \leqslant v_{max}$	$\tilde{v} \leqslant v_a^u$	$v_\epsilon^u \geqslant \tilde{v}$	$\nearrow$	$\nearrow$					(ϵ, v_ϵ^u)
3.3.4.1	$[\bar{w}^u, w_{max}^u)$	$\bar{v} \leqslant v_a^u \leqslant v_{max}$	$\tilde{v} \geqslant v_a^u$		$\searrow$	$\searrow$	$\searrow$	$\searrow$	$\searrow$	$\nearrow$	(a, v_a^u)
3.3.5.1.1	$[w_{max}^u, \infty)$	$v_a^u \geqslant v_{max}$	$\tilde{v} \leqslant v_{max}$	$v_\epsilon^u \leqslant \tilde{v}$	$\searrow$	$\searrow$	$\searrow$	$\searrow$	$\smile$		$(\tilde{w}^u, \tilde{v})$
3.3.5.1.2	$[w_{max}^u, \infty)$	$v_a^u \geqslant v_{max}$	$\tilde{v} \leqslant v_{max}$	$v_\epsilon^u \geqslant \tilde{v}$	$\nearrow$						(ϵ, v_ϵ^u)
3.3.5.1	$[w_{max}^u, \infty)$	$v_a^u \geqslant v_{max}$	$\tilde{v} \geqslant v_{max}$		$\searrow$	$\searrow$	$\searrow$	$\searrow$	$\searrow$		(w_{max}^u, v_{max})

Where $\tilde{w}^u = a - (d - (u - a)\tilde{v})/v_c$.

Table C.24 gives the solution in all possible subcases. □

C.4. Proof of Theorem 5.3

Proof. The result follows from a careful comparison of the cases listed in Table A.11 in Theorem 5.1 and in Table A.12 in Theorem 5.2. □

C.5. Proof of Lemma 5.2

Proof. Proof of part (i) The proof is by contradiction.

Suppose that there exists an optimal solution (denoted by S^*) where the speed on one arc is lower than $\underline{v}$. Without loss of generality, suppose that this arc belongs to the route $(0, \ldots, n+1)$, where $n+1$ is a copy of the depot. Let w_i^* denote the optimal departure time from node i and let v_i^* denote the optimal speed on arc $(i, i+1)$. So there exists $k \in \{0, \ldots, n\}$ such that $v_k^* < \underline{v}$.

The total cost associated with this route is $\sum_{i=0}^n f_c F_i(w_i^*, v_i^*) + d_c W(w_0^*, \ldots, w_n^*, v_0^*, \ldots, v_n^*)$, where F_i denotes the emissions cost on arc $(i, i+1)$ and W is the total time the driver is paid for.

We construct an alternative solution (denoted by S') as follows: let $w_i' = w_i^*$ for $i = 0, \ldots, n$, $v_i' = v_i^*$ for $i = 0, \ldots, k-1, k+1, \ldots, n$ and $v_k' = \underline{v}$. In other words, we increase the speed on arc $(k, k+1)$ to $\underline{v}$ and we keep the same departure time from node $k+1$ (unless $k = n$) by adding some extra waiting time. The resulting solution is feasible since the arrival time at each node is at most equal to that in the optimal solution. Compared to S^*, in S' the total time the driver is paid for (W) can only decrease (it decreases if $k = n$, otherwise it remains the same). Whereas the emissions cost (F_i) is the same on every arc except on arc $(k, k+1)$, where it decreases since $\underline{v}$ is the speed that minimizes the emissions cost for a given departure time in a one-arc problem as shown in Section 5. Therefore, the alternative solution S' yields a total cost lower that the optimal solution S^* and this leads to a contradiction. □

Proof. Proof of part (ii) The proof is by contradiction.

Suppose that there exists an optimal solution (denoted by S^*) where the speed on the first arc of a route is lower than $\min\{\bar{v}, v_{max}\}$. Without loss of generality, suppose that this arc belongs to the route $(0, \ldots, n+1)$, where $n+1$ is a copy of the depot. Let w_i^* denote the optimal departure time from node i and let v_i^* denote the optimal speed on arc $(i, i+1)$. So we have $v_0^* \leqslant \min\{\bar{v}, v_{max}\}$.

The total cost associated with this route is $\sum_{i=0}^n f_c F_i(w_i^*, v_i^*) + d_c W(w_0^*, \ldots, w_n^*, v_0^*, \ldots, v_n^*)$, where F_i denotes the emissions cost on arc $(i, i+1)$ and W is the total time the driver is paid for. This cost function can be rewritten as

$$\sum_{i=1}^n f_c F_i(w_i^*, v_i^*) + d_c W_{1,\ldots,n}(w_1^*, \ldots, w_n^*, v_1^*, \ldots, v_n^*) + f_c F_0(w_0^*, v_0^*) + d_c W_0(w_0^*, v_0^*) \tag{B.2}$$

where $W_{1,\ldots,n}$ is the time spent from the arrival at node 1 until the return to the depot and W_0 is the time spent from the departure from the depot to the arrival at node 1. Note that the last two terms in (B.2) correspond to the total cost function of a one-arc TDPRP when the driver is paid from his departure time.

We construct an alternative solution (denoted by S') as follows: let $w_i' = w_i^*$ for $i = 1, \ldots, n$, $v_i' = v_i^*$ for $i = 1, \ldots, n$, $v_0' = \min\{\bar{v}, v_{max}\}$ and $w_0' > w_0^*$ such that the arrival time at node 1 is the same in S' as in S^*. The departure times and free-flow speeds on arcs $(i, i+1)$ where $i = 1, \ldots, n$ remain unchanged and therefore the resulting solution is feasible. For the same reasons, in both solutions S^* and S' the first two terms of the (B.2) remain the same. Whereas, as results from the proof of Theorem 5.2, the last two terms (B.2) are lower in S' compared to S^*. Hence, we have a contradiction. □

Appendix D. Computational results

D.1. Results on PRP instances

The PRP results in columns 2 and 3 are taken from Demir et al. (2012). The reason behind the slight discrepancy between the values in columns 2 and 4 is due to numerical approximation (see Tables D.25–D.31).

Table D.25
Comparison of PRP versus TDPRP formulations with respect to computational time.

Instance	PRP (£)	*t* (PRP) (s)	TDPRP (£)	*t* (TDPRP) (s)
UK10_01	170.66	163.40	170.66	10.71
UK10_02	204.87	113.90	204.88	3.73
UK10_03	200.33	926.00	200.34	3.36
UK10_04	189.94	396.50	189.95	5.00
UK10_05	175.61	1253.70	175.62	4.93
UK10_06	214.56	347.50	214.53	3.43
UK10_07	190.14	191.00	190.15	5.06
UK10_08	222.16	139.80	222.17	2.23
UK10_09	174.53	54.00	174.54	4.64
UK10_10	189.83	76.00	189.84	2.83
UK10_11	262.07	50.50	262.08	4.40
UK10_12	183.18	1978.70	183.19	14.71
UK10_13	195.97	1235.10	195.97	2.94
UK10_14	163.17	84.10	163.18	2.77
UK10_15	127.15	433.30	127.16	6.25
UK10_16	186.63	680.80	186.63	7.03
UK10_17	159.07	27.00	159.08	3.22
UK10_18	162.09	522.10	162.09	4.19
UK10_19	169.46	130.50	169.46	1.52
UK10_20	168.8	1365.50	168.81	17.44
Average		508.47		5.52

D.2. Results on TDPRP instances

Each table reports the two cases: (i) driver paid from the beginning of the time horizon, (ii) driver paid from his departure time. In both cases the tables display, for each instance, the cost values of the S_D and S_N solutions (denoted by $TC(S_N)$ and $TC(S_D)$) and the CPU times (in s) required to construct these solutions (denoted by $t(S_N)$ and $t(S_D)$). Under the last column are reposted the cost savings of incorporating traffic congestion when planning the vehicles' routes and schedules.

Table D.26
Computational results for 10-node instances with initial congestion period of 3600 s.

Instance	# of vehicles	Drivers paid from the beginning of the time horizon					Drivers paid from departure				
		$TC(S_N)$ (£)	$t(S_N)$ (s)	$TC(S_D)$ (£)	$t(S_D)$ (s)	Saving (%)	$TC(S_N)$ (£)	$t(S_N)$ (s)	$TC(S_D)$ (£)	$t(S_D)$ (s)	Saving (%)
UK10_01	2	Inf.	4.62	183.98	6.01	–	177.97	3.99	168.14	6.05	5.52
UK10_02	2	225.10	3.09	218.90	3.63	2.75	220.26	1.81	203.06	6.79	7.81
UK10_03	2	219.33	12.88	213.34	8.76	2.73	210.54	8.33	197.50	2.94	6.19
UK10_04	2	209.97	2.83	202.17	2.20	3.71	187.18	1.36	185.88	2.65	0.69
UK10_05	2	195.80	3.99	188.07	3.95	3.95	185.77	1.24	172.23	3.27	7.29
UK10_06	2	Inf.	2.55	229.13	3.55	–	Inf.	2.21	213.29	5.86	–
UK10_07	2	210.37	1.54	205.18	3.31	2.47	203.98	1.81	189.34	3.35	7.18
UK10_08	2	242.26	1.83	237.17	2.46	2.1	242.26	1.09	221.33	2.11	8.64
UK10_09	2	194.82	2.59	189.73	2.97	2.61	194.82	2.86	173.89	3.23	10.74
UK10_10	2	210.03	1.91	204.89	2.56	2.44	209.59	2.26	189.05	2.75	9.8
UK10_11	2	Inf.	2.71	277.12	2.57	–	Inf.	1.92	261.28	2.71	–
UK10_12	2	198.41	5.32	193.65	4.20	2.4	181.64	2.52	177.81	3.88	2.11
UK10_13	2	216.19	1.79	208.37	2.08	3.61	205.72	1.18	192.53	2.04	6.41
UK10_14	2	Inf.	1.54	179.84	17.40	–	Inf.	1.20	164.72	6.40	–
UK10_15	2	141.13	3.06	135.46	4.01	4.02	123.22	2.73	119.62	4.39	2.92
UK10_16	2	206.25	4.97	198.86	4.20	3.58	194.80	5.03	183.02	5.60	6.05
UK10_17	2	Inf.	2.17	171.60	2.51	–	Inf.	1.34	155.76	2.81	–
UK10_18	2	182.37	3.78	173.96	6.04	4.61	Inf.	2.90	158.00	4.42	–
UK10_19	2	Inf.	1.74	181.28	5.38	–	Inf.	2.29	165.44	5.61	–
UK10_20	2	189.06	8.37	181.68	11.84	3.9	178.83	14.64	165.84	14.38	7.27

Table D.27
Computational results for 10-node instances with initial congestion period of 7200 s.

Instance	# of vehicles	Drivers paid from the beginning of the time horizon					Drivers paid from departure				
		$TC(S_N)$ (£)	$t(S_N)$ (s)	$TC(S_D)$ (£)	$t(S_D)$ (s)	Saving (%)	$TC(S_N)$ (£)	$t(S_N)$ (s)	$TC(S_D)$ (£)	$t(S_D)$ (s)	Saving (%)
UK10_01	2	Inf.	4.62	201.76	22.61	–	Inf.	3.99	170.08	20.35	–
UK10_02	2	Inf.	3.09	241.31	12.88	–	Inf.	1.81	210.63	23.02	–
UK10_03	2	240.03	12.88	229.69	30.30	4.31	231.47	8.33	198.01	20.99	14.46
UK10_04	2	230.84	2.83	217.56	4.89	5.75	206.4	1.36	185.88	3.54	9.94
UK10_05	2	216.68	3.99	203.91	4.32	5.89	206.71	1.24	172.23	4.36	16.68
UK10_06	2	Inf.	2.55	249.98	6.61	–	Inf.	2.21	218.30	12.38	–
UK10_07	2	231.31	1.54	221.31	5.90	4.32	Inf.	1.81	189.63	3.74	–
UK10_08	2	263.19	1.83	253.01	2.43	3.87	263.19	1.09	221.33	1.96	15.91
UK10_09	2	215.75	2.59	205.57	4.71	4.72	215.75	2.86	173.89	5.06	19.4
UK10_10	2	230.94	1.91	220.74	3.60	4.42	230.53	2.26	189.05	3.82	17.99
UK10_11	2	Inf.	2.71	296.27	3.92	–	Inf.	1.92	264.59	2.92	–
UK10_12	2	219.28	5.32	208.75	21.78	4.80	202.64	2.52	177.81	4.44	12.25
UK10_13	2	Inf.	1.79	224.21	2.94	–	226.65	1.18	192.54	2.63	15.05
UK10_14	2	Inf.	1.54	199.36	5.32	–	Inf.	1.20	167.68	5.44	–
UK10_15	2	Inf.	3.06	152.87	9.70	–	Inf.	2.73	121.19	8.28	–
UK10_16	2	226.95	4.97	214.70	6.53	5.40	215.73	5.03	183.02	6.01	15.16
UK10_17	2	Inf.	2.17	207.46	32.35	–	Inf.	1.34	175.83	16.01	–
UK10_18	2	Inf.	3.78	189.68	11.33	–	Inf.	2.90	158.00	7.03	–
UK10_19	2	Inf.	1.74	199.15	6.48	–	Inf.	2.29	167.47	5.82	–
UK10_20	2	209.99	8.37	197.52	18.80	5.94	197.25	14.64	165.84	12.47	15.92

Table D.28
Computational results for 15-node instances with initial congestion period of 3600 s.

Instance	# of vehicles	Drivers paid from the beginning of the time horizon					Drivers paid from departure				
		$TC(S_N)$ (£)	$t(S_N)$ (s)	$TC(S_D)$ (£)	$t(S_D)$ (s)	Saving (%)	$TC(S_N)$ (£)	$t(S_N)$ (s)	$TC(S_D)$ (£)	$t(S_D)$ (s)	Saving (%)
UK15_01	2	Inf.	234.88	299.06	556.78	–	Inf.	667.67	283.22	618.29	–
UK15_02	2	226	25.92	219.36	30.37	2.94	213.31	28.08	203.52	35.62	4.59
UK15_03	2	Inf.	4746.72	316.59	3186.76	–	Inf.	7422.00	300.75	6316.59	–
UK15_04	3	Inf.	71.64	318.50	53.86	–	Inf.	24.98	294.74	33.26	–
UK15_05	2	Inf.	14.17	299.90	40.14	–	Inf.	41.47	284.06	27.85	–
UK15_06	2	Inf.	8862.00	244.05	1050.61	–	240.6	2221.46	228.21	1932.42	5.15
UK15_07	3	281.15	26.71	269.44	6.44	4.16	261.56	8.19	245.68	9.84	6.07
UK15_08	2	185.47	162.84	178.97	33.59	3.51	171.94	75.11	163.13	52.41	5.12
UK15_09	3	293.51	1138.32	281.89	70.98	3.96	278.86	126.32	258.11	105.38	7.44
UK15_10	2	234.14	40.70	227.71	42.99	2.74	225.05	30.76	211.87	53.35	5.85
UK15_11	2	Inf.	20.69	275.26	232.20	–	Inf.	26.45	259.42	123.38	–
UK15_12	3	340.57	24.63	330.51	19.71	2.95	331.72	38.74	306.75	36.77	7.53
UK15_13	2	Inf.	909.86	265.09	1028.96	–	Inf.	1939.60	249.25	1379.09	–
UK15_14	2	Inf.	3083.37	Inf.	2871.24	–	Inf.	10130.00	Inf.	2408.28	–
UK15_15	2	239.81	48.45	232.81	96.55	2.92	219	134.98	216.97	155.69	0.93
UK15_16	2	224.67	27.34	214.37	7.88	4.58	208.32	7.30	198.53	44.56	4.7
UK15_17	3	Inf.	9.82	302.04	5.00	–	300.07	5.18	278.28	6.25	7.26
UK15_18	3	Inf.	58.39	332.40	10.29	–	Inf.	27.24	308.65	21.24	–
UK15_19	2	184.85	9.46	178.31	4.50	3.54	176.81	4.24	162.47	6.81	8.11
UK15_20	3	Inf.	16.28	220.57	7.10	–	Inf.	2.84	196.81	9.42	–

Table D.29
Computational results for 15-node instances with initial congestion period of 7200 s.

Instance	# of vehicles	Drivers paid from the beginning of the time horizon					Drivers paid from departure				
		$TC(S_N)$ (£)	$t(S_N)$ (s)	$TC(S_D)$ (£)	$t(S_D)$ (s)	Saving (%)	$TC(S_N)$ (£)	$t(S_N)$ (s)	$TC(S_D)$ (£)	$t(S_D)$ (s)	Saving (%)
UK15_01	2	Inf.	234.68	337.71	2489.17	–	Inf.	667.67	306.42	2972.56	–
UK15_02	2	Inf.	25.86	235.40	63.91	–	231.96	28.08	203.72	42.19	12.17
UK15_03	2	Inf.	4858.37	Inf.	476.42	–	Inf.	7422.00	Inf.	748.03	–
UK15_04	3	Inf.	71.58	343.16	67.64	–	Inf.	24.98	295.64	194.17	–
UK15_05	2	Inf.	14.14	349.49	272.13	–	Inf.	41.47	331.04	520.05	–
UK15_06	2	Inf.	8856.99	263.74	1853.29	–	Inf.	2221.46	232.06	2105.63	–
UK15_07	3	Inf.	26.68	304.60	168.01	–	Inf.	8.19	257.08	114.88	–
UK15_08	2	206.04	162.79	194.81	70.76	5.45	192.87	75.11	163.13	60.50	15.42
UK15_09	3	Inf.	1137.68	306.18	234.59	–	Inf.	126.32	258.66	290.29	–
UK15_10	2	Inf.	40.65	245.23	74.02	–	Inf.	30.76	213.55	44.76	–
UK15_11	2	Inf.	20.68	337.12	824.14	–	Inf.	26.45	308.15	790.05	–
UK15_12	3	Inf.	24.61	354.41	31.77	–	Inf.	38.74	69.55	72.18	–
UK15_13	2	Inf.	913.76	282.77	2093.01	–	Inf.	1939.60	262.93	5685.92	–
UK15_14	2	Inf.	3079.17	Inf.	6.48	–	Inf.	10130.00	Inf.	6.63	–
UK15_15	2	260.51	48.30	248.65	94.52	4.55	Inf.	134.98	216.97	106.01	–
UK15_16	2	245.24	27.30	230.21	11.01	6.13	Inf.	7.30	198.53	12.89	13.40
UK15_17	3	Inf.	9.80	325.80	14.14	–	Inf.	5.18	278.28	14.34	16.10
UK15_18	3	Inf.	58.32	363.74	173.09	–	Inf.	27.24	316.22	417.77	–
UK15_19	2	202.42	9.47	194.15	13.23	4.09	197.74	4.24	162.47	10.80	17.84
UK15_20	3	Inf.	16.23	244.55	243.15	–	Inf.	2.84	200.68	71.21	–

Table D.30
Computational results for 20-node instances with initial congestion period of 3600 s.

Instance	# of vehicles	Drivers paid from the beginning of the time horizon					Drivers paid from departure				
		$TC(S_N)$ (£)	$t(S_N)$ (s)	$TC(S_D)$ (£)	$t(S_D)$ (s)	Saving (%)	$TC(S_N)$ (£)	$t(S_N)$ (s)	$TC(S_D)$ (£)	$t(S_D)$ (s)	Saving (%)
UK20_01	3	347.16	416.29	337.9	265.72	2.68	328.90	212.49	314.10	169.66	4.50
UK20_02	3	365.84	295.04	352.9	225.98	3.54	Inf.	321.04	329.12	161.04	–
UK20_03	3	233.27	76.69	224.0	44.97	3.97	216.53	66.35	200.01	42.36	7.63
UK20_04	3	354.83	3360.44	347.1	1546.29	2.17	354.34	2929.29	323.36	1919.35	8.74
UK20_05	3	325.59	258.29	317.4	360.26	2.53	312.87	370.71	292.12	219.98	6.63
UK20_06	3	349.35[a]	2124.82	365.02[a]	5637.66	–	339.50[a]	6701.12	347.27[a]	1520.50	
UK20_07	3	255.39	1456.06	246.93[a]	2394.83	–	223.1[a]	10800.40	223.4[a]	1091.46	–
UK20_08	3	307.47	575.73	298.3	54.03	3.00	288.17	232.23	274.10	83.39	4.88
UK20_09	3	Inf.	54.36	345.0	169.47	–	Inf.	32.64	321.26	119.14	–
UK20_10	3	291.58[a]	3977.5	310.9	1816.07	–	307.98	9120.02	287.15	2288.59	6.76
UK20_11	3	391	140.35	381.6	38.50	2.41	374.23	173.63	357.82	234.21	4.38
UK20_12	3	346.02	2253.71	334.6	463.88	3.29	322.48	1853.51	310.87	463.90	3.60
UK20_13	3	339.15	83.24	329.9	176.90	2.74	327.46	128.74	306.10	74.62	6.52
UK20_14	3	Inf.[a]	10799.6	Inf.[a]	1701.06	–	Inf.[a]	2521.06	Inf.[a]	1651.95	–
UK20_15	3	349.63	642.49	338.4	607.60	3.22	327.47	3105.17	313.94	800.90	4.13
UK20_16	3	358.16	741.31	346.4	170.18	3.30	331.72	895.87	322.60	149.28	2.75
UK20_17	3	Inf.	905.97	379.72[a]	2170.39	–	Inf.	2498.11	355.61	5864.80	–
UK20_18	3	Inf.	445.71	367.5	1132.39	–	Inf.	1357.34	343.71	685.20	–
UK20_19	3	351.16	1926.32	343.4	3405.90	2.22	349.63	253.10	319.60	2524.09	8.59
UK20_20	3	354.13	11.56	343.1	15.56	3.11	337.82	10.09	319.37	13.75	5.46

[a] Not solved to optimality.

Table D.31
Computational results for 20-node instances with initial congestion period of 7200 s.

Instance	# of vehicles	Drivers paid from the beginning of the time horizon					Drivers paid from departure				
		$TC(S_N)$ (£)	$t(S_N)$ (s)	$TC(S_D)$ (£)	$t(S_D)$ (s)	Saving (%)	$TC(S_N)$ (£)	$t(S_N)$ (s)	$TC(S_D)$ (£)	$t(S_D)$ (s)	Saving (%)
UK20_01	3	Inf.	416.29	362.44	286.10	–	Inf.	212.49	314.90	673.14	–
UK20_02	3	Inf.	295.04	378.75	207.29	–	Inf.	321.04	331.20	541.94	–
UK20_03	3	264.38	76.69	247.53	158.97	6.37	245.9	66.35	200.00	100.15	18.66
UK20_04	3	Inf.	3360.44	371.80	4318.09	–	Inf.	2929.29	324.30	4647.32	–
UK20_05	3	356.9	258.29	340.60	894.88	4.57	Inf.	370.71	293.10	940.19	–
UK20_06	3	349.35[a]	2124.82	412.04[a]	10799.80	–	339.50[a]	6701.12	Inf.	–	–
UK20_07	3	285.35	1456.06	270.63[a]	7058.32	–	223.17[a]	10800.40	Inf.[a]	4299.49	–
UK20_08	3	338.8	575.73	321.91	128.01	4.99	Inf.	232.23	274.40	119.65	–
UK20_09	3	Inf.	54.36	379.15	676.14	–	Inf.	32.64	331.80	1761.27	–
UK20_10	3	291.58[a]	3977.50	335.73[a]	4271.10	–	Inf.	9120.02	288.80	7355.26	–
UK20_11	3	Inf.	140.35	414.64	2554.09	–	Inf.	173.63	368.20	2471.30	–
UK20_12	3	Inf.	2253.71	361.30	3523.84	–	Inf.	1853.51	316.20	3076.75	–
UK20_13	3	Inf.	83.24	360.09	2171.69	–	Inf.	128.74	312.60	1884.26	–
UK20_14	3	Inf.[a]	10799.60	Inf.[a]	1954.92	–	Inf.[a]	2521.06	Inf.[a]	1779.78	–
UK20_15	3	Inf.	642.49	366.01	3407.18	–	Inf.	3105.17	318.50	5048.37	–
UK20_16	3	Inf.	741.31	370.12	748.19	–	363.12	895.87	322.60	1811.35	11.16
UK20_17	3	Inf.	905.97	410.747[a]	10800.80	–	Inf.	2498.11	369.13[a]	10797.90	–
UK20_18	3	Inf.	445.71	395.57	4054.01	–	Inf.	1357.34	351.65[a]	10799.50	–
UK20_19	3	Inf.	1926.32	371.63	9726.61	–	Inf.	253.10	324.111[a]	10799.50	–
UK20_20	3	Inf.	11.56	367.51	21.24	–	Inf.	10.09	320.00	36.21	–

[a] Not solved to optimality.

References

Barth, M., Boriboonsomsin, K., 2008. Real-world CO_2 impacts of traffic congestion. Transportation Research Record: Journal of the Transportation Research Board 2058, 163–171.

Barth, M., Younglove, T., Scora, G., 2005. Development of a Heavy-Duty Diesel Modal Emissions and Fuel Consumption Model. Technical Report. UCB-ITS-PRR-2005-1, California PATH Program, Institute of Transportation Studies, University of California at Berkeley.

Bektaş, T., Laporte, G., 2011. The Pollution-Routing Problem. Transportation Research Part B 45 (8), 1232–1250.

Conrad, R.G., Figliozzi, M.A., 2010. Algorithms to quantify impact of congestion on time-dependent real-world urban freight distribution networks. Transportation Research Record: Journal of the Transportation Research Board 2168, 104–113.

Cordeau, J.-F., Laporte, G., Savelsbergh, M.W.P., Vigo, D., 2007. Vehicle routing. In: Barnhart, C., Laporte, G. (Eds.), Transportation, Handbooks in Operations Research and Management Science, vol. 14. Elsevier, Amsterdam, The Netherlands, pp. 367–428 (Ch. 6).

Demir, E., Bektaş, T., Laporte, G., 2011. A comparative analysis of several vehicle emission models for freight transportation. Transportation Research Part D: Transport and Environment 6 (5), 347–357.

Demir, E., Bektaş, T., Laporte, G., 2012. An adaptive large neighborhood search heuristic for the Pollution-Routing Problem. European Journal of Operational Research 223 (2), 346–359.

Figliozzi, M.A., 2010. Vehicle routing problem for emissions minimization. Transportation Research Record: Journal of the Transportation Research Board 2197, 1–7.

Figliozzi, M.A., 2011. The impacts of congestion on time-definitive urban freight distribution networks CO_2 emission levels: Results from a case study in Portland, Oregon. Transportation Research Part C: Emerging Technologies 19, 766–778.

Franceschetti, A., Honhon D., Van Woensel, T., Bektaş, T., Laporte G., 2013. The Departure Time and Speed Optimization Problem. Technical Report. Eindhoven University of Technology.

Hansen, S., Byrd, A., Delcambre, A., Rodriguez, A., Matthews, S., Bertini, R.L., 2005. PORTAL: An on-line regional transportation data archive with transportation system management applications. In: 2005 CITE Quad/WCTA Regional Conference, April 7–9, 2005. Vancouver, BC, Canada.

Hickman, J., Hassel, D., Joumard, R., Samaras, Z., Sorenson, S., 1999. Technical Report. MEET Methodology for Calculating Transport Emissions and Energy Consumption <http://www.transport-research.info/Upload/Documents/200310/meet.pdf> (accessed 28.01.13).

Hvattum, L.M., Norstad, I., Fagerholt, K., Laporte, G., 2013. Analysis of an exact algorithm for the vessel speed optimization problem. Networks 62 (2) 132–135.

International Road Transport Union, 2012. Congestion is Responsible for Wasted Fuel <http://www.iru.org/en_policy_co2_response_wasted> (accessed 28.01.13).

Jabali, O., Van Woensel, T., de Kok, A.G., 2012. Analysis of travel times and CO_2 emissions in time-dependent vehicle routing. Production and Operations Management 21 (6), 1060–1074.

Knight, R. (Ed.), 2004. Technical Report. Mobility 2030: Meeting the challenges to sustainability <http://www.is.wayne.edu/drbowen/SenSemF04/Mobility2030FullReport.pdf> (accessed 28.01.13).

Maden, W., Eglese, R., Black, D., 2010. Vehicle routing and scheduling with time-varying data: a case study. Journal of the Operational Research Society 61 (3), 515–522.

Norstad, I., Fagerholt, K., Laporte, G., 2010. Tramp ship routing and scheduling with speed optimization. Transportation Research Part C: Emerging Technologies 19 (5), 853–865.

Sbihi, A., Eglese, R., 2007. Combinatorial optimization and green logistics. 4OR: Quarterly Journal of Operations Research 5 (2), 99–116.

Tol, R.S.J., 2005. The marginal damage costs of carbon dioxide emissions: an assessment of the uncertainties. Energy Policy 33 (16), 2064–2074.

Van Woensel, T., Creten, R., Vandaele, N., 2001. Managing the environmental externalities of traffic logistics: the issue of emissions. Production and Operations Management 10 (2), 207–223.

Van Woensel, T., Kerbache, L., Peremans, H., Vandaele, N., 2008. Vehicle routing with dynamic travel times: a queueing approach. European Journal of Operational Research 186 (3), 990–1007.

Wikipedia, 2012. Rush Hour <http://en.wikipedia.org/wiki/Rush_hour> (accessed on 28.01.13).